Tribology International 133 (2019) 246–262

Contents lists available at ScienceDirect

Tribology International

journal homepage: www.elsevier.com/locate/triboint

The effect of over-based calcium sulfonate detergent additives on white etching crack (WEC) formation in rolling contact fatigue tested 100Cr6 steel

A.D. Richardson[a,*], M.-H. Evans[a], L. Wang[a], M. Ingram[b], Z. Rowland[a], G. Llanos[a], R.J.K. Wood[a]

[a] nCATS, Faculty of Engineering and Physical Sciences, University of Southampton, UK
[b] Afton Chemical Ltd, Bracknell, UK

ARTICLE INFO

Keywords:
White etching cracks
Hydrogen diffusion
Additive chemistry
Tribofilm analysis

ABSTRACT

Over-based calcium sulfonate (OBCaSul) additives in oils are considered potentially critical in driving WEC formations, this 'driving' effect being unclear. Rolling contact fatigue testing of 100Cr6 steel using FE8 and PCS Micro-Pitting-Rig lubricated with oils containing varying OBCaSul concentrations have been conducted, tested samples being analysed using serial sectioning, Thermal desorption analysis (TDA) to measure hydrogen diffusion, and SEM/EDX of the tribofilms formed. Results show that OBCaSul concentration appears to affect WEC formation propensity, a reversal relationship of formations being shown between test rigs. Evidence shows oils containing OBCaSul form thick Ca dominated tribofilms, potentially promoting hydrogen diffusion and WEC formations in the FE8 rollers, where thinner Zn—S tribofilms on the FE8 raceways may demote hydrogen diffusion and WEC formations.

1. Introduction

Premature failures of wind turbine gearbox bearings (WTGBs) cause significant downtime and high repair costs causing substantial impact to the wind energy industry. One of the most noted failure modes of WTGBs is that of White Structure Flaking (WSF) due to the formation of White Etching Cracks (WECs) typically ~ 1 mm below the contact surface, WECs being associated with a microstructural alteration known as White Etching Area (WEA).

Driving mechanisms for WSF and WECs have been debated for a number of years and a consensus into what the major influencing factor is has yet to be decided. One specific factor is the effect of additive chemistry and in addition, the effect additive chemistry has on the generation and diffusion of hydrogen, as a prominent driver for WSF and WECs. Additives found in lubricants that have been shown to reduce RCF life and promote WSF include; greases and lubricants containing sulphur-phosphorous extreme-pressure/anti-wear (EP/AW) additives, such as zinc dithiophosphates (ZDDP/ZnDTP/ZnDDP) and detergent/rust preventatives such as calcium sulfonates [1–10]. Hydrogen poisoning sulphur can aid in hydrogen diffusion by inhibiting molecular hydrogen recombination [11], where decomposition of EP/AW additives such as ZDDPs at nascent catalytic surfaces can generate hydrogen [12,13].

A number of studies conducted by the authors of this manuscript and others have used an automotive gear oil known to be 'bad' and rapidly promote WECs [3,6,14–19], this oil containing Over-based calcium sulfonate (OBCaSul) and AW ZDDP additives. This oil causes bearing failure on the FAG-FE8 test rig between 16 and 40 h [14,18,20] in contrast to the 1000 h test under the same conditions without WSF, where a pure base oil was used [20]. FAG-FE8 testing conducted by the authors using this oil has shown that the diffusible hydrogen measured in the test rollers increased with RCF test duration, where this was coupled with an increase in WEC formations [21]. FAG-FE8 testing has shown that oils containing ZDDP, without the introduction of metal or non-metal additives formed WECs, addition of Ca/Na sulfonates also formed WECs as well as Ca/Na in the absence of ZDDP [5]. It is also noted that FAG-FE8 tests have created cracks using a mineral oil without any 'considerable' oil additives [22].

Calcium sulfonate detergents and more specifically OBCaSul are typically used in automotive gear oils; therefore, most of the literature focuses on their impact on AW performance of engine components for the automotive industry. Calcium sulfonate detergents are used to keep metal surfaces clean by forming a protective layer as well possessing good AW/EP, friction reducing and anti-scuffing properties. ZDDP decomposition rates have been found to be retarded by the OBCaSul detergents since the reaction between ZDDP and OBCaSul is proposed to be antagonistic to the performance of the AW tribofilm [23]. OBCaSul are suggested to have an antagonistic effect toward sulphur containing species in film formation, OBCaSul inhibiting ZDDP tribofilm formation [24–26], creating 'patchy/weakened' heterogeneous ZDDP tribofilms

* Corresponding author.
E-mail address: A.D.Richardson@soton.ac.uk (A.D. Richardson).

https://doi.org/10.1016/j.triboint.2019.01.005
Received 7 September 2018; Received in revised form 20 December 2018; Accepted 4 January 2019
Available online 07 January 2019
0301-679X/

[26–30] and potentially aiding in hydrogen diffusion processes by promoting and prolonging nascent surface exposure [31].

A number of suggestions explaining the antagonistic effect of OBCaSul are as follows; OBCaSul inhibits the formation of a ZDDP film due to the formation of a colloid dispersion with ZDDP [32]. OBCaSul competition with ZDDP at the contact surface in the formation of a tribofilm, the OBCaSul breaks down to form carbonate, which is deposited on the metal surface [33]. It has been shown from multiple surface techniques that Ca displaces the Zn polyphosphates in the AW film [34,35], OBCaSul may inhibit polyphosphate chain formation by formation of Ca phosphate [36]. X-ray absorption near-edge structure spectroscopy (XANES) has shown that mix of ZDDP and OBCaSul resulted in the formation of considerable Ca phosphate in the film [37]. The over-basing component is suggested to retard the rate-determining step of AW action (decomposition stage) of ZDDP [38], however, others suggest that it can improve AW performance by forming a 'paste-like' structure in the contact [39,40].

Based on past literature, it is considered that the OBCaSul in the 'bad' oil mentioned above is the critical additive driving WEC formations, this 'driving' effect being unclear, where this study aims to investigate this. To accomplish this, rolling contact fatigue (RCF) testing of 100Cr6 steel using FAG-FE8 and PCS-MPR test rigs, lubricated with the 'bad' oil and purposely-formulated oils containing varying wt% of OBCaSul additive have been conducted. The tested samples have been examined and analysed using serial sectioning techniques, Thermal desorption analysis (TDA), and SEM/EDX of the tribofilms formed (RCF testing, serial sectioning, and TDA for the FE8 tests lubricated with the 'bad' oil are from previous studies conducted by the authors [18,21], and are used for comparison in this study). By using these techniques, the effect that oils containing OBCaSul additives have on the tribofilm formed in the contact, diffusion of hydrogen into the steel during operation, and WEC formations has been investigated, where the effect that these additive have on tribofilm and hydrogen diffusion influencing WEC formations have been explored.

2. Materials, techniques and experimental methods

2.1. FAG-FE8

Testing was conducted on a standard FAG-FE8 rig, comprehensive details of which can be seen in Ref. [18]. The test conditions (with the exception of the oils used) can be found in Ref. [18]. The tested bearing raceway are pre-roughened before testing to R_q value of 0.5 μm. As illustrated in Ref. [18], the centre of the raceway track and rollers experiences pure rolling with rising slip of up to ± 12.5% slide-roll-ratio (SRR) along the contact major axis towards the edges. The rollers experience both – ve and + ve directional slip due to being sandwiched between two raceways.

Four tests were conducted in total using an oil specifically formulated for this study containing Group III ISO VG 68 with ZDDP AW additive, where the OBCaSul detergent wt% in the oil for each of the four tests was altered (ZDDP only (0% OBCaSul), 1.4%, 2.8% and 5.6%), base oil and ZDDP staying constant. Tests were shut down manually at 18 h to keep duration constant between tests. The calculated maximum Hertzian contact pressure Pmax is in the range of ~1.5–1.9 GPa.

Initial minimum oil film thickness (h_{min}) between rollers and raceways is calculated using the Hamrock and Dowson equation [41,42]. Lambda ratio (λ) is calculated based upon h_{min} and the roughness (R_q) values given in Ref. [18], the bearing has been run under boundary lubrication. Oil temperature in the contact is controlled at 100 °C.

2.2. Micro-Pitting Rig (MPR)

Testing was also conducted on a PCS-Micro-Pitting Rig (MPR) (Fig. 1) so that a comparative assessment between the MPR and FAG-FE8 rigs on WEC formations could be made. The MPR is a computer controlled RCF rig in which three equal diameter counterface rings are in contact with a smaller diameter roller positioned in the middle of the rings. The three rings have a diameter of 54 mm and the test roller is 12 mm with a 1 mm wide wear track (Fig. 1 (c)). Rings and rollers are AISI 52100 martensitically through hardened steel. Chemical composition of the roller and rings can be found in Ref. [3]. Rollers and rings have a Rockwell C hardness of 60 (746 HV) and 63 (867 HV) respectively [3]. Servo controlled motors control the rings and roller separately to allow for testing at different SRR. Lubricant is supplied to the contact through a dip lubrication system. A motorised ball screw applies load, which acts through an arm. A piezoelectric accelerometer is used to measure vibration in the contact during operation, once a threshold is reached the test is stopped automatically.

Five tests were conducted using the same four OBCaSul oils tested on the FAG-FE8 as detailed above, and a fully formulated semi-synthetic gear oil (Oil X) that contains ZDDP and OBCaSul 2.8% which is known to be 'bad' and promote WEC formations (full details can be found in Ref. [18]). The water content of these oils was also measured pre-RCF testing using Karl Fischer titration (see Table 1). All tests were run to 18 h before being shutdown manually. The calculated Hertzian contact pressure P_{max} is 1.9 GPa. Subsurface shear stresses have been calculated using Hertzian contact theory. The SRR during operation is set at - 30%. The test conditions of the five tests are given in Table 2.

Initial minimum oil film thickness (h_{min}) between the rings and roller has been calculated using the Hamrock and Dowson visco-elastic equation [41,42]. Lambda ratio (λ) has been calculated based upon h_{min} and the roughness (R_q) values given in Table 2. Oil temperature is kept at 100 °C during operation as is measured by a probe inserted into the test chamber.

2.3. Contact surface inspection and subsurface examination using metallographic analysis

All tested sample surfaces were initially inspected using optical macroscopy. For the FAG-FE8 test samples, images were taken at 60° intervals around the circumference of the rollers. For the MPR samples, images were taken at 120° intervals around the circumference of the rollers. Example images of the contact surface for each test can be seen in Fig. 3.

Metallographic analysis was then conducted to record individual WECs and associated damage features in all the RCF tested samples

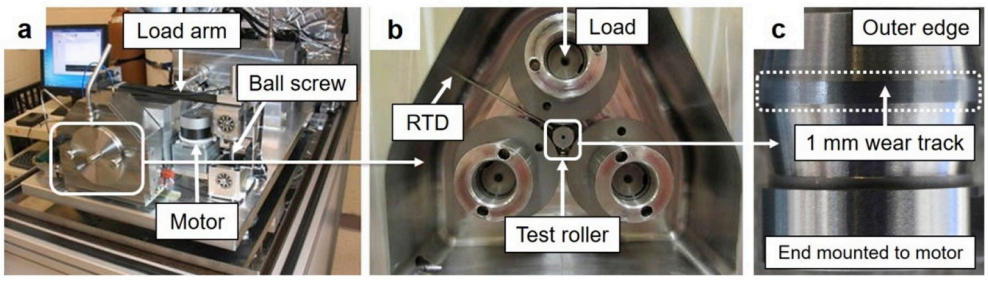

Fig. 1. MPR set-up. (a) Overview of MPR test rig. (b) Inside the test cell. RTD denotes Resistance temperature detector. (c) Test roller. (a) and (b) adapted from Ref. [3]. (a) and (b) Reprinted and adapted by permission from Springer Nature: Springer, Tribology Letters, The Influence of sliding and contact severity on the generation of white etching cracks, Gould, B. and A. Greco, Copyright (2015), https://link.springer.com/journal/11249.

Table 1
Water content (ppm) for the tested oils pre-RCF test.

Test Oil	Water content (ppm)
ZDDP only (OBCaSul 0%)	40
OBCaSul 1.4%	83
OBCaSul 2.8%	87
OBCaSul 5.6%	175
Oil X (OBCaSul 2.8%)	209

Table 2
MPR test conditions.

Test specimen dimension	
Test Roller	Diameter 12 mm
Test Rings	Diameter 54 mm
Oil properties	
Oil type	Group III ISO VG 68 with ZDDP anti-wear and OBCaSul detergent (varied between 0 and 5.6%) additives
Viscosity	62 cSt (40 °C), 10.23 cSt (100 °C)
Pressure viscosity coefficient (α)	1.6E-08 Pa^{-1}
Dynamic viscosity η_o (100 °C)	8.7E-03 Pa*S
Bearing material properties	
Rings/roller	Martensitic AISI 52100 steel/Martensitic AISI 52100 steel
Hardness roller/rings	746 HV/867 HV
Surface roughness (R_a) rings/roller	0.1–0.15 μm/0.1–0.2 μm
Test conditions	
Rolling speed (m/s)	3.4 m/s
Load (N)	500 N
SRR (%)	−30%
Max contact pressure (P_{max})	~1.9 GPa
Bearing/oil temperature (°C)	100 °C
Minimum film thickness (h_{min})	0.125 μm
Lambda ratio (λ)	λ = 0.5–0.8 (depending on Ra used)
Test durations	
Test number (all 18 h) 1/2/3/4/5	ZDDP only (0% OBCaSul), 1.4% OBCaSul, 2.8% OBCaSul, 5.6% OBCaSul, and Oil X
Subsurface shear stresses	
Max orthogonal shear stress ($\tau_{o,\ max}$)	~495 MPa (acting @ a depth below the contact surface of ~80 μm)
Max unidirectional shear stress ($\tau_{uni,\ max}$)	~602 MPa (acting @ a depth below the contact surface of ~126 μm)

from both FAG-FE8 and MPR testing using the same procedures as detailed in Ref. [18]. For the FAG-FE8 tests, rollers were prepared in the same way as in Ref. [18]. The MPR test roller were prepared in a similar way, the single test roller being analysed. Rollers were mounted such that they were sectioned in the axial direction from the outer roller edge (see Fig. 1 (c)). Details of the sectioning analysis for FAG-FE8 and MPR samples are given below.

2.3.1. FAG-FE8

Macro sectioning (at 50 μm per slice material removal rate) was first conducted on rollers from all the tests from the outer edge of the rollers until the point where WECs were first found. This was then followed by coarse serial sectioning (at average material removal rate of ~30, 35 and 38 μm per slice depending on the test). This is deemed a suitable sectioning removal rate to catch the majority of WECs including smaller networks; however, very small WECs may have been missed due to the slice removal rates. Imaging of WECs was taken at every five slices. Inclusions were recorded during sectioning. Inclusions may have been missed due to the sectioning removal rates conducted, where inclusions observed in the FAG-FE8 rollers are typically small in size (typically ~ 2–15 μm) [18]. The individual sectioning ranges (sectioning start and stop range) and removal rates (μm/sectioning slice) for each test are listed in Table 3. Oil X data is from Ref. [18], data for Oil X rollers given in Table 3 is for an 18 h test for comparison. Fig. 2 details the sectioning analysis procedure.

2.3.2. MPR

Careful material removal was first conducted on all tests from the outer edge of the roller up until the edge of the wear scar at ~3.5 mm (no contact between roller and rings before this point). Once completed, fine serial sectioning was started (~4.3–7.4 μm per slice depending on the test). Imaging of WECs was taken at every five slices. Inclusion-WEC interactions were recorded during sectioning. The individual sectioning interval ranges and removal rates for each test are listed in Table 3. Fig. 2 details the sectioning analysis procedure.

2.4. Thermal desorption analysis (TDA)

To measure the hydrogen content in the tested samples, that may have diffused into and been trapped in the steel during RCF testing, TDA was performed for the samples from the FAG-FE8 tests using two different experimental set-ups under BS ISO 3690 standards [43] as detailed in Ref. [21].

2.5. Tribofilm analysis

The rollers and raceways from FAG-FE8 testing have been analysed using SEM/EDX to check the tribofilms formed on the contact surface during operation. The MPR samples were not analysed in this study. Tribofilms formed by ZDDP only (0%), OBCaSul (1.4%–5.6%) and Oil X have been examined, where for Oil X the tribofilms formed at 2, 6 and 18 h RCF test durations have been examined (Oil X RCF testing is from Ref. [18]). Prior to the analysis, samples are rinsed in heptane, isopropyl alcohol and blow-dried. 5 kV accelerating voltage is used for the analysis. The estimated tribofilm thickness is calculated based upon an empirical power fit of 100 + MTM-Slim analyses spanning ashless and ZDDP AW tribofilms. The fit is developed between a normalisation

Table 3
Sectioning intervals and removal rates conducted during the metallographic analysis.

Test Oil	Nº samples analysed		Sectioning range (start and stop positions) (~mm)				Removal rate (~μm/slice)	
			Macro sectioning/material removal		Serial sectioning		Serial sectioning	
	FAG-FE8	MPR	FAG-FE8	MPR	FAG-FE8	MPR	FAG-FE8	MPR
ZDDP only (OBCaSul 0%)	3x Rollers	1x Roller	Avg: 0–1.52	0–3.5	Avg: 1.52–3.0	3.5–3.8	Avg: 35	4.3
OBCaSul 1.4%	3x Rollers	1x Roller	Avg: 0–2.01	0–3.5	Avg: 2.01–3.0	3.5–3.8	Avg: 30	4.3
OBCaSul 2.8%	3x Rollers	1x Roller	Avg: 0–2.04	0–3.5	Avg: 2.04–3.0	3.5–3.8	Avg: 30	4.3
OBCaSul 5.6%	3x Rollers	1x Roller	Avg: 0–1.52	0–3.5	Avg: 1.52–3.0	3.5–3.8	Avg: 38	7.4
Oil X [18]*	3x Rollers	1x Roller	Avg: 0–1.85	0–3.5	Avg: 1.85–3.0	3.5–3.8	Avg: 3.6 or 15	7.4

KEY:For the FAG-FE8 rollers, macro sectioning at ~ 50 μm slice intervals is conducted at the start from the outer roller edge (0.00 mm) until the first visible sign of WECs are found in any one test roller. For the MPR roller, careful material removal from the outer roller edge (0.00 mm) until the edge of the wear track is reached (at ~3.5 mm) was conducted. **Note 1:** for the FAG-FE8 rollers, sectioning ranges and removal rates are given as an average across the 3x analysed rollers. ***Note 2:** data for Oil X FAG-FE8 is from Ref. [18], this data is from an 18 h FE8 test for comparison.

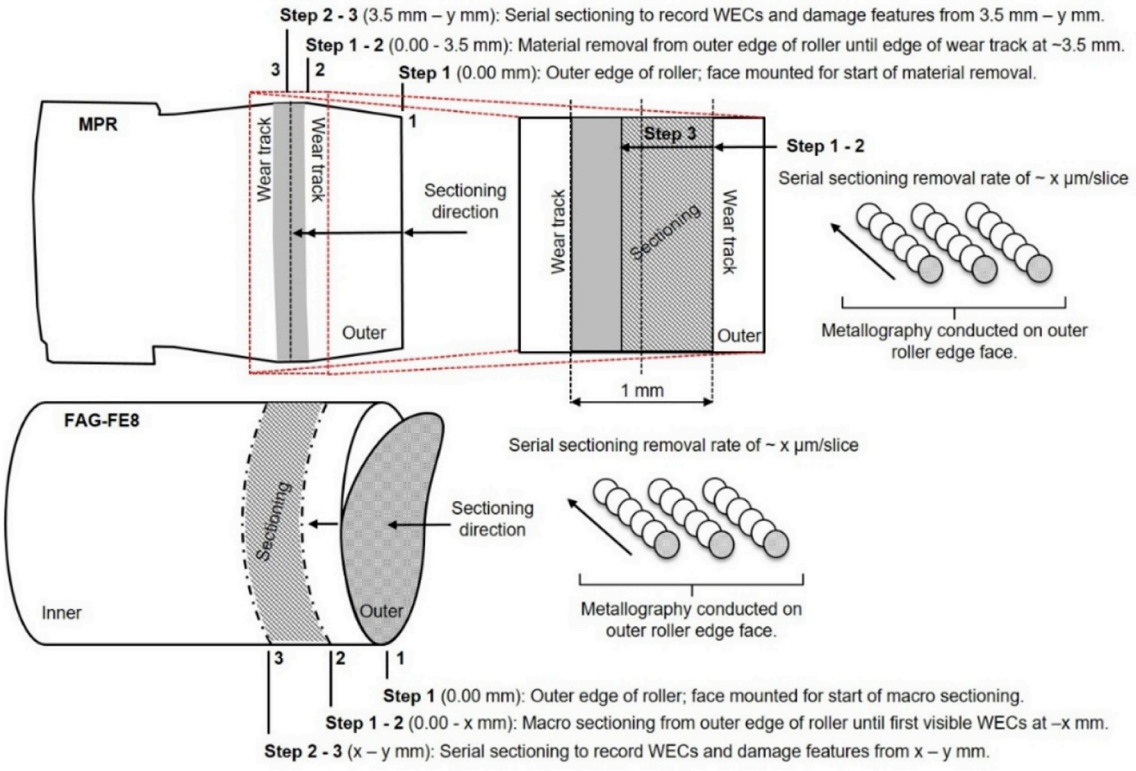

Fig. 2. Details of the sectioning procedure for the FAG-FE8 and MPR tests.

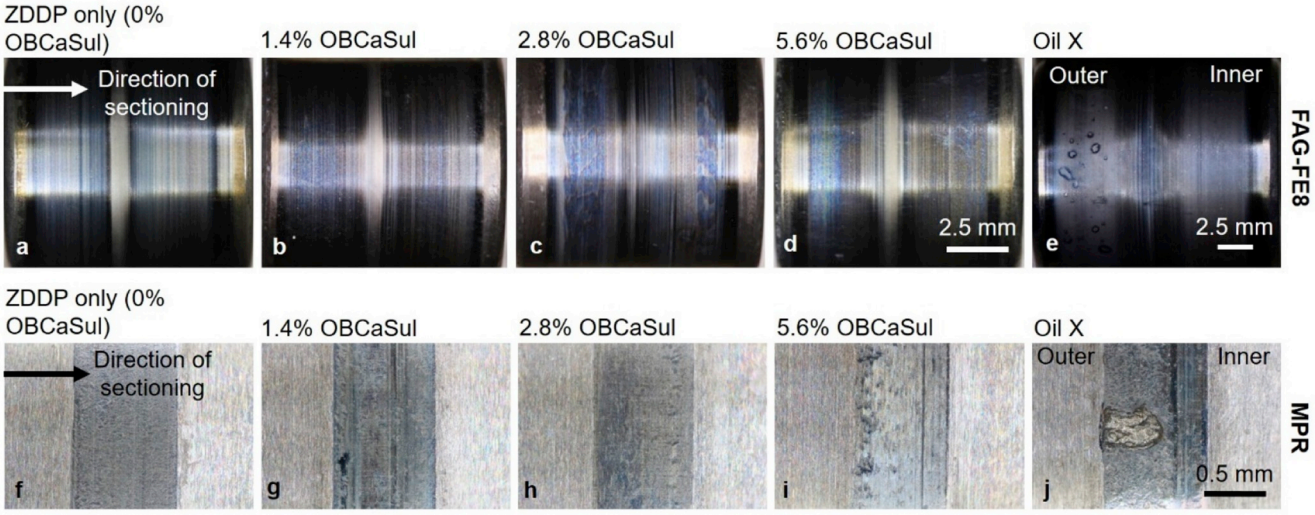

Fig. 3. Optical macroscope images of rollers from each test for the FE8-FAG and MPR test rigs. Images (a)–(e) show one of the 60° interval zones around the circumference of the roller for the FE8-FAG tests, for Oil X see Ref. [18]. Images (f)–(j) show one of the 120° interval zones around the circumference of the roller for the MPR tests.

factor for the 100 + tests and the tribofilm thickness when measured by the MTM-Slim. For the FAG-FE8 analysed tribofilms, no corresponding MTM-Slim data was available; therefore, the normalisation factor is used to get an estimate.

3. Results

3.1. Contact surface inspection

3.1.1. FAG-FE8

Wear across the rollers is observed on both sides of the central pure rolling region corresponding to outer and inner zones (Fig. 3). No visible signs of spalling were seen on any of the rollers except that from Oil X test. Mild wear is observed on the ZDDP only (OBCaSul 0%) and OBCaSul 1.4% tests with a slight increase seen for OBCaSul 2.8% and 5.6%. Oil X [18] in comparison showed visible signs of damage on the surface in the form of dents/impressions, no signs of spalling were found on the rollers sectioned, however, spalling was observed on other rollers from the same bearing.

3.1.2. MPR

Only Oil X showed visible signs of spalling damage (Fig. 3 (j)). Wear and micropiting are observed on all rollers from the OBCaSul oil tests.

Table 4
Summary of serial sectioning results.

Test oil	WECs recorded		Surface connections		Inclusion interactions	
	FAG-FE8	MPR	FAG-FE8	MPR	FAG-FE8	MPR
ZDDP only (OBCaSul 0%)	Total: 0	Total: 49 Total SF: 21	Total: 0	Total: 1	Total: 0	Total: 12, Total: 11*
OBCaSul 1.4%	Total: 0	Total: 27 Total SF: 9	Total: 0	Total: 2	Total: 0	Total: 7, Total: 6*
OBCaSul 2.8%	Total: 17 Total SF: 15	Total: 0	Total: 5	Total: 0	Total: 2, Total: 2*	Total: 0
OBCaSul 5.6%	Total: 12 Total SF: 8	Total: 0	Total: 0	Total: 0	Total: 10, Total: 10*	Total: 0
Oil X [18]*	Total: 119 Total SF: 63	Total: 27 Total SF: 18	Total: 16	Total: 2	Total: 50, Total: 30*	Total: 7, Total: 7*

Key: *Total number of inclusion-WEC interactions ranked high likelihood (1 or 2) of initiation (see Appendix A for details on ranking system). ***Note 1:** data for Oil X FAG-FE8 is from Ref. [18], this data is from an 18 h test for comparison. **Note 2:** for the FAG-FE8 tests, the 'Total' number of WECs recorded is the total across all 3x analysed rollers, for the MPR this is across the 1x analysed roller. **Total SF** denotes the total number of WECs recorded that started and finished within the sectioning range i.e. recorded in the entirety.

3.2. Metallographic analysis

An overview of the FAG-FE8 and MPR tests results, including numbers of WECs, NMIs interacted with WECs and whether the WECs have surface connections, is summarised in Table 4. Inclusions were evaluated using a ranking system described in Appendix A.

Examples of NMIs found to have interacted with WECs are shown in Fig. 4, where the corresponding information of the inclusion type, size, location and test oil type is provided. As it can be seen, from the MPR testing, inclusions observed in the OBCaSul 0%, 1.4% and Oil X are small (average size at ~3–11 μm, ~2–8 μm and ~3–13 μm respectively) and are either globular sulfide-oxides (D_{Dup}), globular oxide (D) of manganese sulphide or manganese duplex (A). For the FAG-FE8 tests, the inclusions have been previously observed in the rollers as either globular sulfide-oxides (D_{Dup}) and globular oxide (D) based upon extensive collection of inclusion results [18]. Due to the size of the serial sectioning rates (15–38 μm) conducted on the rollers from the ZDDP only (OBCaSul 0%) and OBCaSul (1.4%–5.6%) oils tests in this study, it was not possible to gather clear data on the length of inclusions. However, since the same type of bearings are used; it is assumed similar type and size of inclusions present in the rollers from the ZDDP only (OBCaSul 0%) and OBCaSul (1.4%–5.6%) oil tests.

The spatial distributions and depth of inclusion-WEC interactions for the FAG-FE8 and MPR tests are shown in Fig. 5.

During the serial sectioning processes, where possible, the dimension and location of individual WECs was observed and have been recorded, the results from the FAG-FE8 and MPR tests are summarised in Fig. 6.

3.3. Thermal desorption analysis

Both rollers and the raceways from the FAG-FE8 tests have been analysed to measure the content of diffusible hydrogen, and the TDA results are summarised below and in Table 5 and Figs. 8 and 9 (TDA results for Oil X are from Ref. [21]). TDA results from set-up 1 (Fig. 8) have shown that.

- Elevated concentrations of diffusible hydrogen were measured in the rollers.
- An increase in diffusible hydrogen is measured for increase in OBCaSul (1.4%–5.6%).
- ZDDP only oil (OBCaSul 0%) showed average hydrogen concentration of 0.37 ppm.
- For both TDA setups, diffusible hydrogen contents in raceway sections are found to be negligible across all oils (close to the detection limit of the instrument) and are similar to that of the untested (0-h) control rollers.
- Higher water content (ppm) coupled with higher concentrations of diffusible hydrogen measured.

TDA set-up 2 (Fig. 9) has shown that.

- Elevated concentrations of diffusible hydrogen measured for ZDDP only oil (OBCaSul 0%) and OBCaSul 5.6% w.r.t untested (0-h) control rollers.
- For Oil X rollers and raceways, hydrogen desorbs out from the start of the analysis, this being later (250–300 min) for the OBCaSul 0% and 5.6% oils at a temperature range of ~125–150 °C.
- A single desorption peak is seen at ~250–300 °C for the ZDDP only oil (OBCaSul 0%) and OBCaSul 5.6% oil roller and raceways, this being much shallower for the raceways.

3.4. Tribofilm analysis

Tribofilm analysis results using SEM/EDX on rollers and raceways from FAG-FE8 testing are summarised in Figs. 10–14 and Table B1–B3 in Appendix B. EDX results of the film formed across the axial contact length of rollers and width of the wear track on the raceways for Oil X (2, 6 and 18 h) are shown in Fig. 10, and the corresponding results for the ZDDP only (0%) and OBCaSul (1.4%–5.6%) oils are shown in Fig. 11. Estimated tribofilm thicknesses are presented in Fig. 12. Figs. 13 and 14 present EDX phase maps for Oil X (2, 6 and 18 h) rollers and raceways.

4. Discussion

4.1. Oil chemistry influence on WEC formations

4.1.1. WEC formation propensity

A significant difference in propensity and size of WEC formations is found for Oil X compared to the ZDDP only (OBCaSul 0%) and OBCaSul (1.4%–5.6%) oils (see Table 4 and Fig. 6 and 7), thus the different oil chemistry of Oil X promotes WEC formations more so than OBCaSul oils. ZDDP only oil (OBCaSul 0%) when tested on the FE8 showed no WECs (see Table 4 and Fig. 6), conversely, when tested on the MPR rig, this is the most detrimental oil to WEC size and propensity (see Table 4 and Figs. 6 and 7).

For the FE8 rollers, an increase in OBCaSul wt% from 1.4% to 2.8% and 5.6% resulted in a jump from zero WECs recorded to a number of WECs being recorded (17 and 12 WECs recorded for the 2.8% and 5.6% oils respectively) (see Table 4 and Fig. 6). Further testing with different wt% of OBCaSul between 1.4% and 2.8% should be conducted to

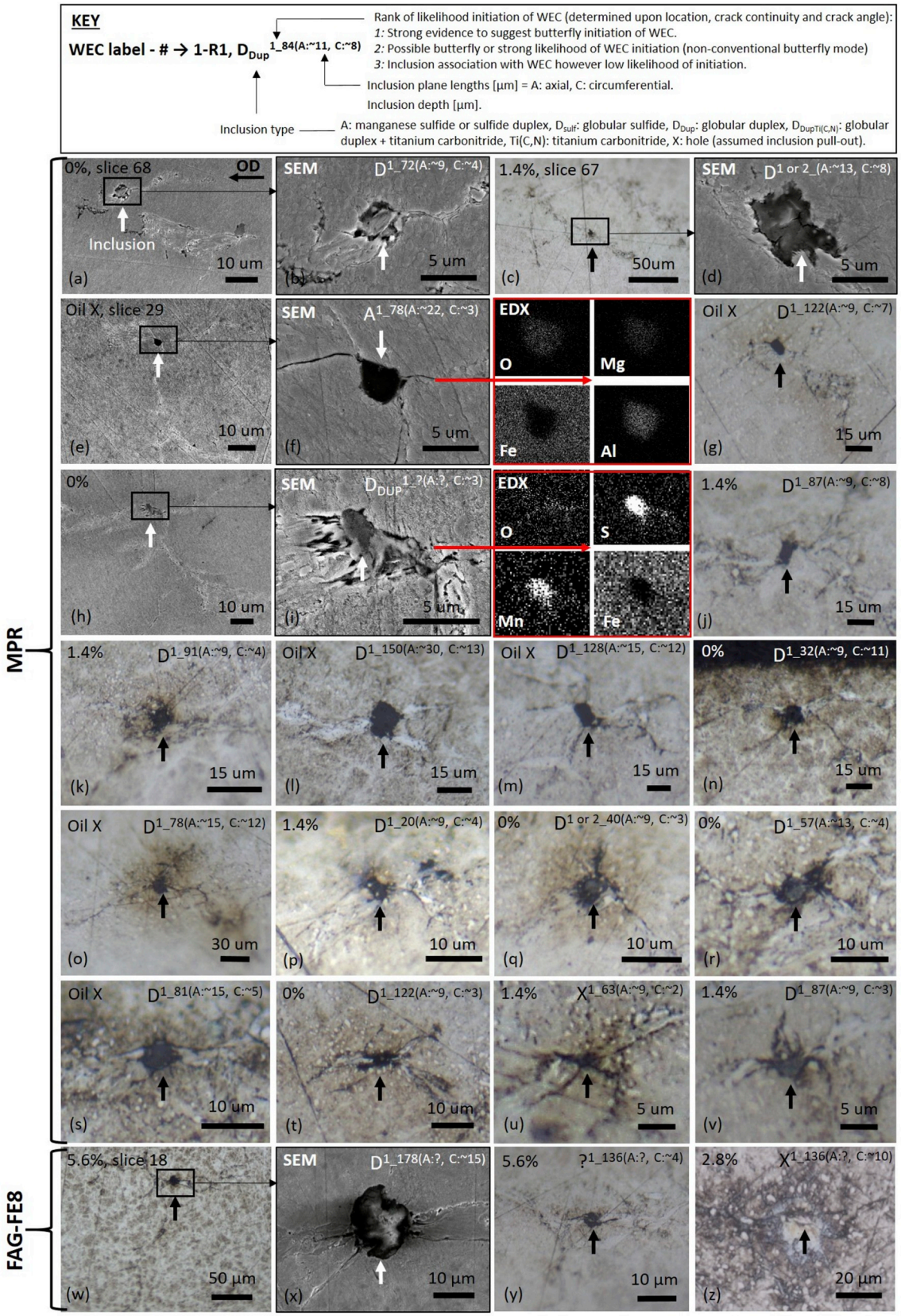

Fig. 4. Images of typical inclusion-WEC interactions recorded in the MPR and FAG-FE8 analysed rollers. The white and black arrows indicate the inclusion in each case. A key above the images details how to interpret the inclusion-WEC interaction information in each case. See Appendix A for more details on the ranking system.

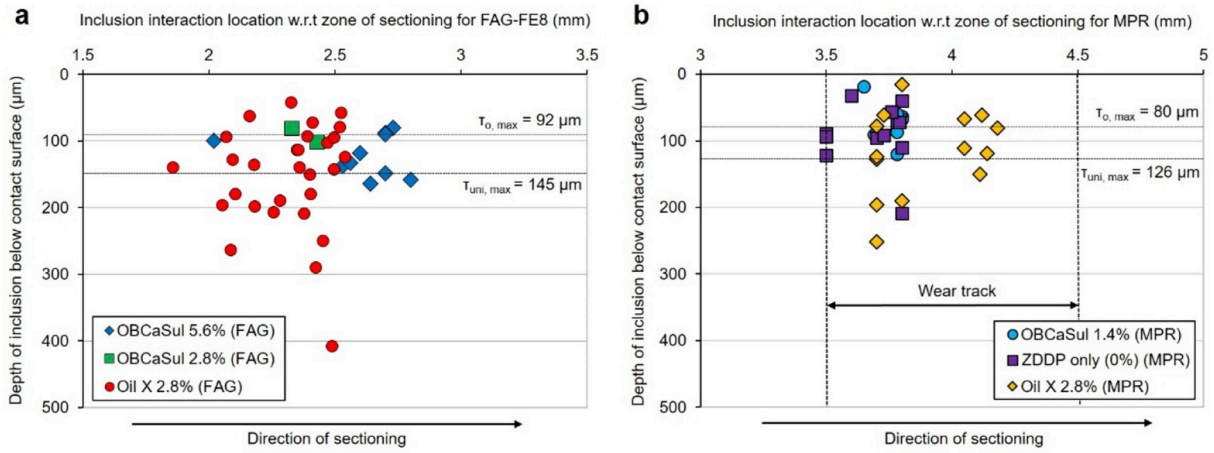

Fig. 5. Spatial distribution of inclusion-WEC interactions. (a) FAG-FE8 with respective zone of maximum subsurface shear stress, Oil X data from Ref. [18]. (b) MPR with respective zones of maximum subsurface shear stress.

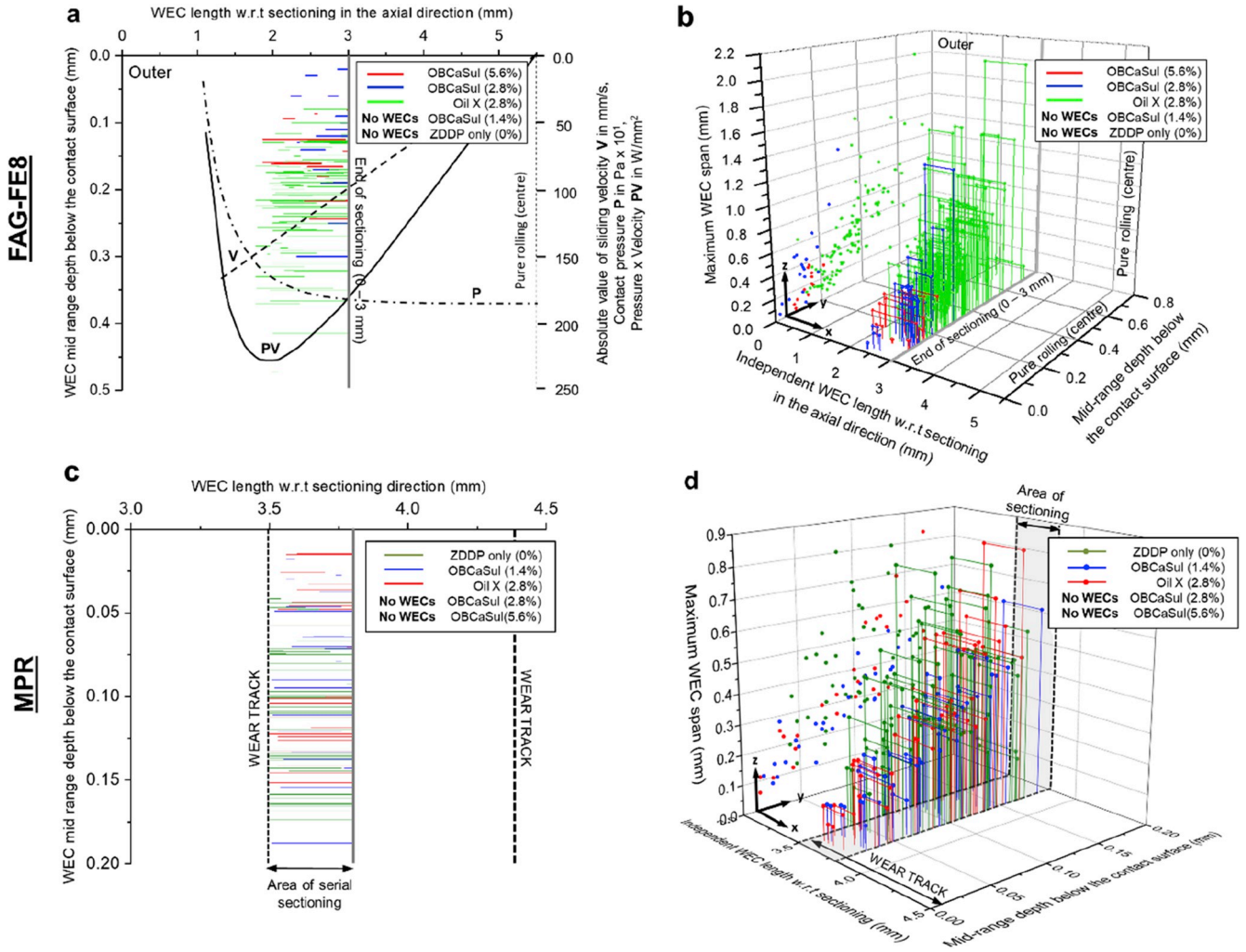

Fig. 6. (a) and (c) Distribution of individual WECs recorded in FE8 and MPR rollers respectively across the area of sectioning with corresponding WEC mid-range depth below the contact surface (0.00 mm) (y-axis). (a) Shows pressure P, absolute sliding velocity V, and slip energy PV superimposed onto the plot for the FE8 tests (adapted from Ref. [16]). (b) and (d) 3D plot of recorded WECs in the FE8 and MPR tested rollers respectively. X-axis: axial length of the roller (FE8: 0–5.5 mm and MPR: 3–4.5 mm). Y-axis: mid-range depth below the contact surface (0.00 mm). Z-axis: max span of individual WECs (see Fig. 7 for details). YZ-projection dots represent the position of each independent WEC in the Y-axis and Z-axis. For FAG-FE8 testing, note that Oil X data is taken from Ref. [18] and presented here for comparison.

Table 5
Concentration of diffusible hydrogen (ppm) measured by TDA using set-up 1 and 2.

Bearing section	0 h (ctrl)		ZDDP only (OBCaSul 0%)		1.4% OBCaSul		2.8% OBCaSul		5.6% OBCaSul		[a]Oil X @ 18 h [21]	
Set-up 1 (TDA @ 400 °C), Set-up 2 (TDA to 300 °C @ 25 °C/hr) concentrations in ppm												
Roller	SU 1	SU 2	SU 1	SU 2	SU 1	SU 2	SU 1	SU 2	SU 1	SU 2	SU 1	SU 2
1x Roller		0.40	0.39, 0.31, 0.40	0.36, 0.58	0.25, 0.24, 0.37	–	0.35, 0.43, 0.45	–	0.60, 0.40, 0.45, 0.50	0.46, 0.63		0.78
[b]Multiple roller combinations	0.12										[b]Avg: 0.50	
Raceway												
1x Section	0.07	0.32	0.02	0.12	0.16	–	0.13	–	0.09	0.23		0.29
[c]Multiple raceway section combinations											[c]Avg: 0.09	

KEY:All samples with non-spalled contact surfaces unless otherwise stated. **SU 1 or SU 2** denotes setup 1 or setup 2.
[a] TDA results for Oil X at 2, 4, 6, 12 and 16.5 h are detailed in Ref. [21].
[b] Average concentration from multiple Oil X 18 h rollers (combinations of 1, 2, 3x rollers and 2x inner and outer roller halves).
[c] Average concentration from multiple Oil X 18 h raceway sections (combinations of 1 and 2x sections).

examine if any trend in WEC propensity exists between these wt%. For an increase in OBCaSul wt% from 2.8% to 5.6%, although no great difference in number of WECs were recorded, WECs were found to be on average longer for the 5.6% oil (see Figs. 6 and 7).

The opposite is seen in OBCaSul wt% versus number of WEC for the MPR tests, a decrease in OBCaSul from 2.8% to 1.4% resulted in a jump from no WECs recorded to several WECs being recorded (see Table 4 and Fig. 6), the 5.6% oil also showing no WECs. Testing of OBCaSul wt % below 1.4% but more than 0 wt% should be conducted to see if there is any trend for decrease in WEC propensity. It is suggested that the opposite behaviour between the FAG-FE8 and MPR tests may be due to differences in the rigs respective contact dynamics influencing the behaviour of OBCaSul, where differences may include.

(i) Slip – On the FAG-FE8 at the centre of bearing contact exists a pure rolling region, with rising slip of up to ± 12.5% SRR along the contact major axis, corresponding to slip regions on the roller/raceway. The MPR tests on the other hand run at −30% SRR, calculated 'frictional energy accumulation' [16] is thus far greater for the MPR (300%) compared to the FAG-FE8 (100%) [44]. It is noted, however, that lubricant factors are not accounted for in the energy accumulation model [44]. Frictional energy accumulation in areas of high slip [16] and resultant higher hydrogen adsorption are proposed to lead to higher concentrations below the surface resulting in WEC failures.
(ii) Contact conditions - smaller area of contact for the MPR in comparison to the FAG-FE8, where for the MPR case it is proposed through modelling that the smaller contact area allows for less hydrogen diffusion/penetration and a faster escape rate due to the surrounding 'out of contact' area [44].
(iii) Contact cycles and 'regeneration time' - (the time between subsequent contact cycles, rollers being slightly longer than the raceways in the FE8 case), where longer regeneration times lead to longer WEC lives [16]. This is considered to be due to lower frictional energy accumulation and influence on surface film formation, which in turn may affect hydrogen diffusion.

It was also suspected that the differences in lubrication chemistry between the tested oils could affect the tribofilm formed during RCF operation (this is discussed in **4.4** of this paper), where contact dynamics/conditions could effect this, in turn potentially playing a role in hydrogen diffusion, and WEC formations.

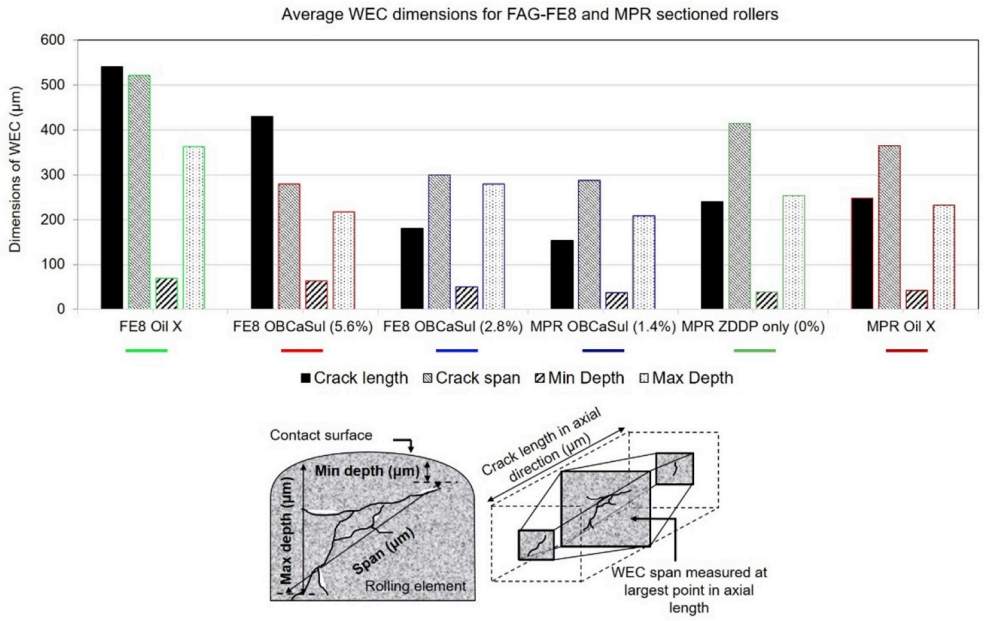

Fig. 7. Average dimensions for the FAG-FE8 and MPR recorded WECs. Note no WECs were recorded in rollers from the FE8 OBCaSul (1.4%), FE8 ZDDP only (0%), MPR OBCaSul (2.8%), and MPR OBCaSul (5.6%) tests. FAG-FE8 Oil X data is from Ref. [18].

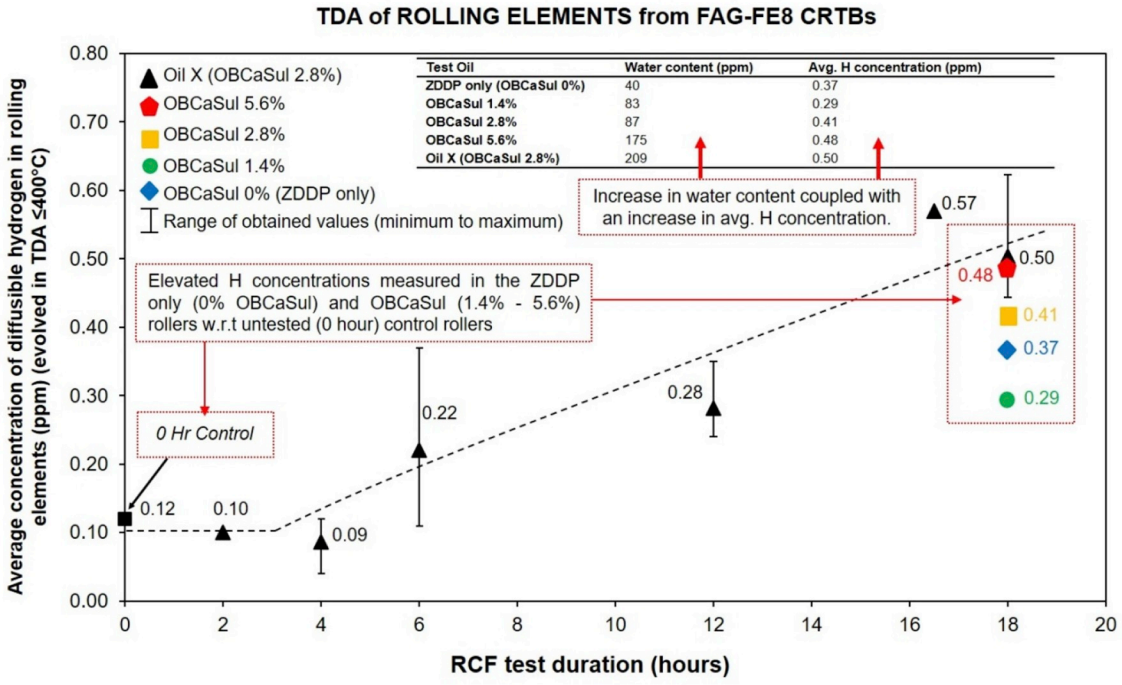

Fig. 8. Thermal desorption analysis (set-up 1 TDA @ 400 °C) of rollers from FAG-FE8 ZDDP only (OBCaSul 0%) and OBCaSul (1.4%–5.6%) tested oils and Oil X. Oil X TDA data is from Ref. [21]. Diffusible hydrogen concentrations in ZDDP only (OBCaSul 0%) and OBCaSul (1.4%–5.6%) oil tested rollers (all run to 18 h), superimposed onto the measured concentrations for Oil X tested rollers on the FAG-FE8 rig.

WECs recorded in the FAG-FE8 rollers across all oils fall within the zones (around ~ 2 mm zone) of high slip energy (PVmax, see Fig. 6). It has been identified previously by the authors on serial sectioning analysis of the FE8 Oil X rollers [18], that this zone is where the highest propensity for WEC initiations exists (as shown in Fig. 6).

4.1.2. Subsurface or surface initiation of WECs

The vast majority of WECs recorded in the FAG-FE8 rollers across all oils were contained entirely within the subsurface and without connection to the contact surface, therefore surface initiation of these WECs is infeasible (Table 4). Any interaction/connections to the surface

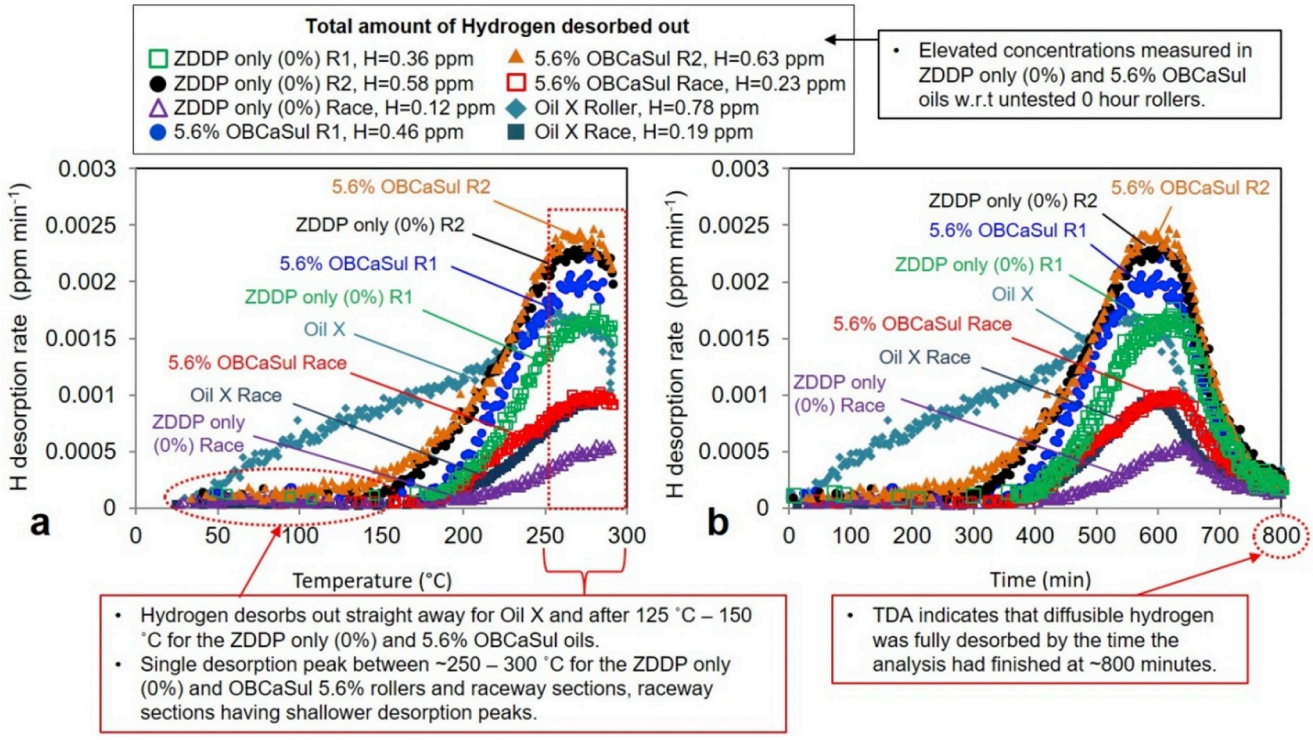

Fig. 9. Hydrogen desorption curves for FAG-FE8 ZDDP only (0%), 5.6% OBCaSul and Oil X (18 h only) RCF tested bearings using TDA set-up 2 (ramped TDA to 300 °C including the total diffusible hydrogen concentration measured. (a) Hydrogen desorption rate (ppm/minute) vs. desorption temperature (°C). (b) Hydrogen desorption rate (ppm/minute) vs. analysis time (minutes). See Table 5 for individual TDA measurements. Note: Data for Oil X is from Ref. [21].

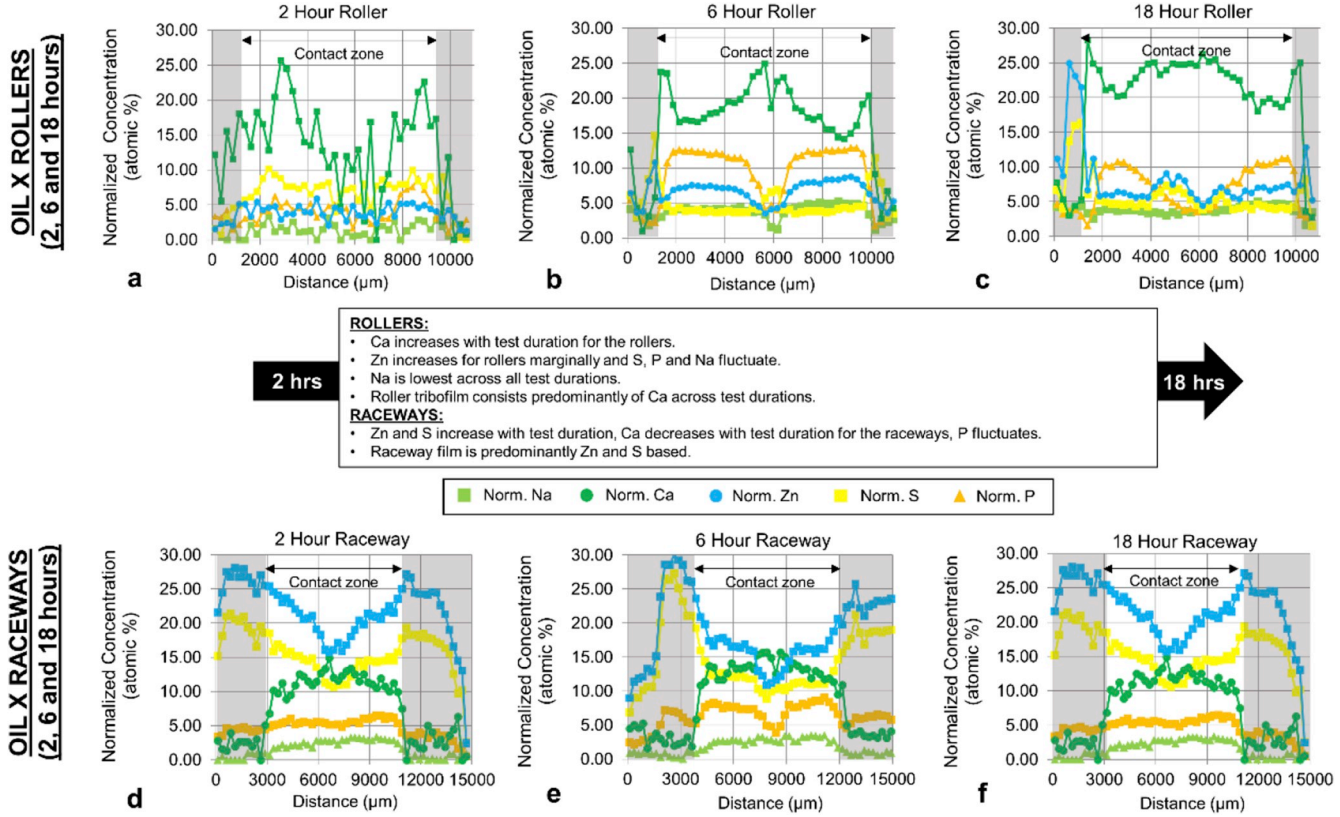

Fig. 10. EDX analysis of the RCF tested Oil X normalised tribofilms formed in the approximate roller/raceway contact zone across 2, 6 and 18-h. (a–c) rollers and (d–f) raceways.

made were predominantly small/short in size relative to the size of the WEC network. Only five cases of interaction/connection to the contact surface were recorded for WECs across all oils tested on the MPR rig (Table 4), connections again being small/short in size. It must be noted that for any WECs that had not started and finished within the sectioning range, interactions/connections still may exist, and further

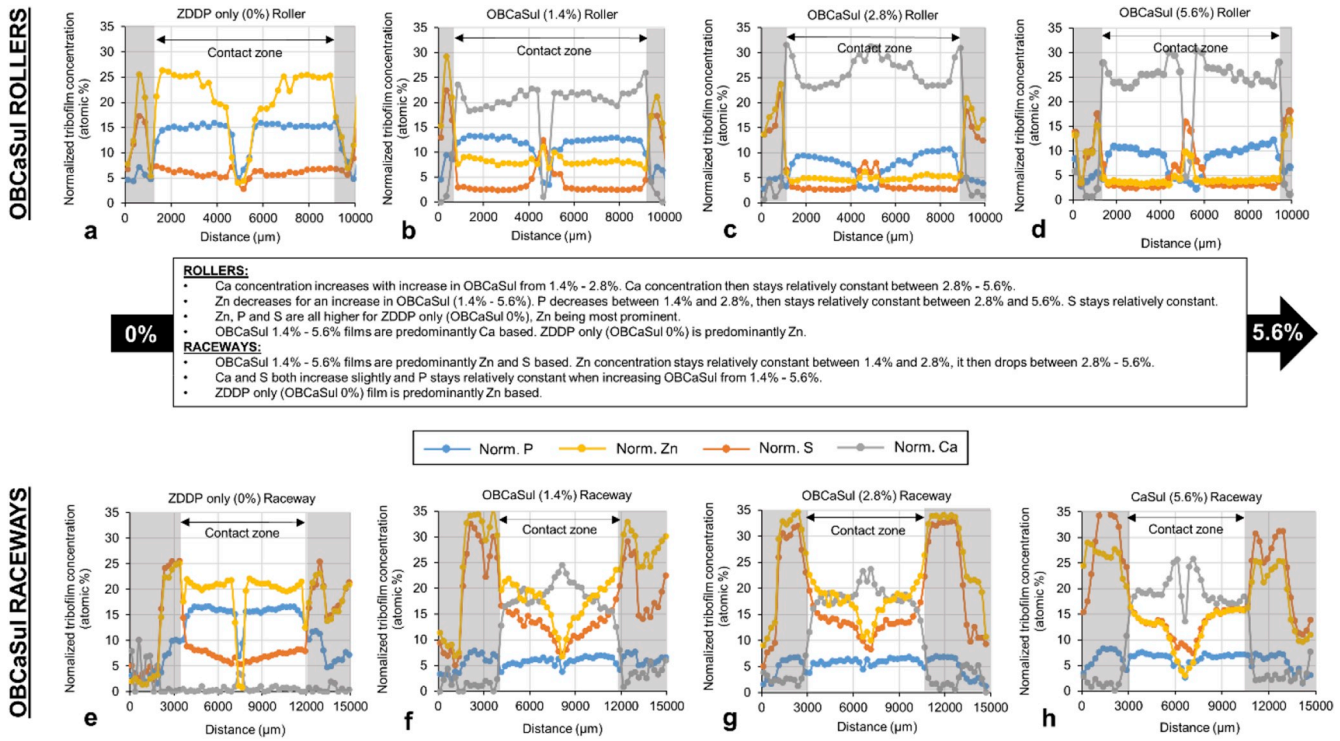

Fig. 11. EDX analysis of normalised tribofilms formed in the approximate roller/raceway contact zone for RCF tested ZDDP only (OBCaSul 0%) and OBCaSul (1.4%–5.6%) oils. (a) ZDDP only (OBCaSul 0%) roller. (b–d) OBCaSul 1.4%–5.6% rollers. (e) ZDDP only (OBCaSul 0%) raceways. (f–g) OBCaSul 1.4%–5.6% raceways.

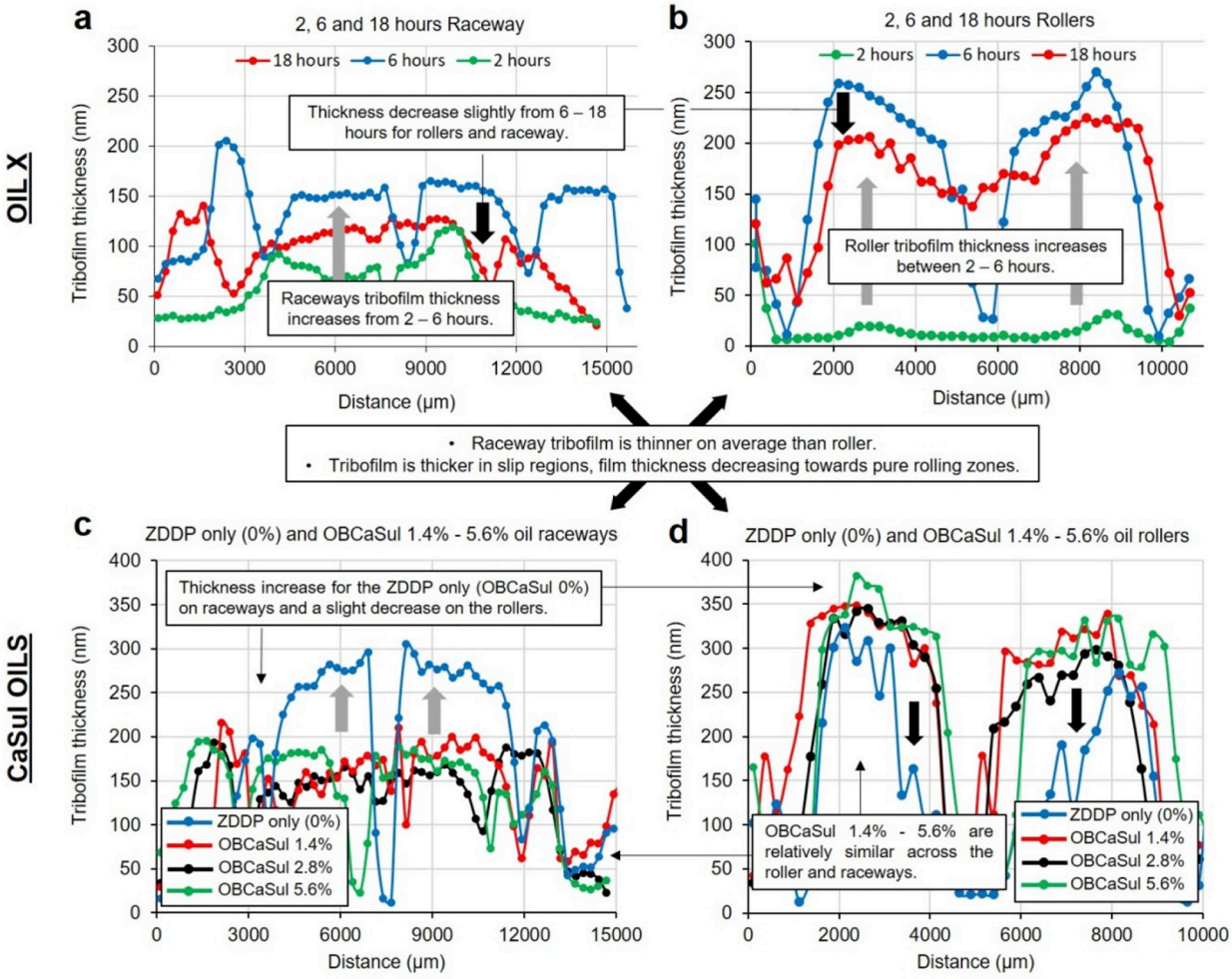

Fig. 12. Estimated tribofilm thickness from SEM/EDX analysis. (a–b) Oil X 2, 6 and 18 h and (c–d) OBCaSul 0%–5.6%.

sectioning would be needed to confirm this.

A number of inclusion-WEC interactions have been recorded in the OBCaSul oil rollers (see Table 4 and see Fig. 4 for examples). Inclusions recorded are small/short in size (FE8: ~2–20 μm, and MPR: ~2–13 μm) and being predominantly globular sulfide-oxides (D_{Dup}), globular oxide (D) or manganese sulfide/sulfide duplex (A) (A type only recorded in MPR rollers) in type. For the FAG-FE8, inclusion-WEC interactions recorded in the OBCaSul oil rollers are within a similar size range and type to the inclusion-WEC interactions recorded in the Oil X rollers [18]. It is considered that a number of inclusions may have been missed in the OBCaSul oils due to size of the sectioning removal rates (~15–38 μm) conducted relative to the small size of the inclusions. A far greater number of inclusion-WEC interactions have been recorded in the FAG-FE8 Oil X rollers in comparison to the OBCaSul (1.4%–5.6%) oils (see Table 4). This is proposed to be due to (i) smaller removal rates (~3–5 μm); therefore, more chance to 'catch' WEC-inclusion interactions; (ii) higher number of WECs recorded in the Oil X rollers, thus more inclusion interactions; (iii) specific lubricant chemistry of Oil X allowing inclusion initiation to occur more easily.

Given the evidence, one mechanism for WEC initiation and propagation for the FAG-FE8 and MPR tested oils is in the subsurface, where differences in lubrication chemistries between the tested oils has not affected this. This further verifies the author's previous findings on FAG-FE8 testing using Oil X [1,18] and other works by the authors [45–47] that WECs can initiate and propagate entirely within the subsurface. In contrast to the results found in this paper and previous works by the authors of this study [14,18], where WECs were recorded in the FE8 rollers only, in Ref. [22], as well as cracks also being recorded in FE8 raceways, cracks found in the FE8 raceways and rollers are proposed to originate from the surface in high slide regions, initiated by local high stresses at asperity contacts due to the rollers high surface roughness (it is noted that rollers were intentionally not ground to achieve a high surface roughness and intentionally embrittled through high temperature austenisation), cracks subsequently propagating into the subsurface toward the zone of maximum subsurface shear stress. WECs have been created and recorded previously through MPR testing [3,4] however, the authors of this manuscript point out that conclusive evidence on whether WECs initiated at the surface/subsurface or interacted with inclusions cannot be made, since 3D mapping of WECs in their entirety was not conducted. This study shows conclusively that subsurface initiation and propagation can be one mechanism in the MPR tests.

In addition, evidence from this study further verifies the author's previous revelations that subsurface initiation is highly likely at small/short non-metallic inclusions [1,18,45–47]. Again, differences in lubrication chemistries between the tested oils has not affected this. For the FAG-FE8 case this is strongly supported, since inclusion-WEC interactions have been recorded at the infant stages of their evolution [18]; however, for the MPR case, this would require further sectioning analysis to catch inclusion-WEC at the early stages.

4.2. Influence of oil chemistry on hydrogen diffusion

Discussions are focused on FE8 testing only. Due to time

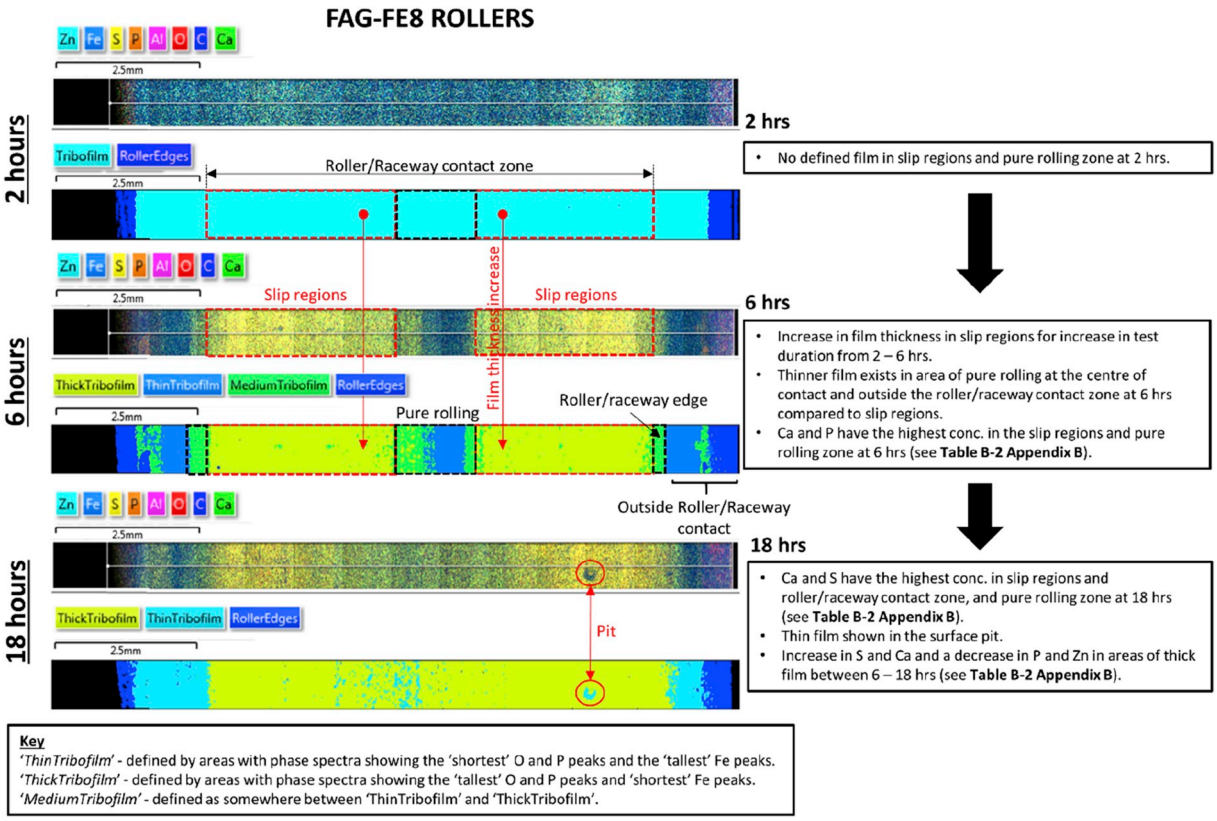

Fig. 13. EDX phase maps for Oil X rollers across 2, 6 and 18 h. Key explains difference between thickness terms.

considerations, TDA was not conducted on the MPR rollers.

TDA for set-up 1 has shown that oils containing OBCaSul with ZDDP, and ZDDP only oils have allowed the diffusion of hydrogen into the FE8 steel rollers during RCF operation and not the raceways (negligible concentrations measured similar to untested '0 h control' samples) (Table 5 and Fig. 8). Differences in oil chemistry, therefore, having

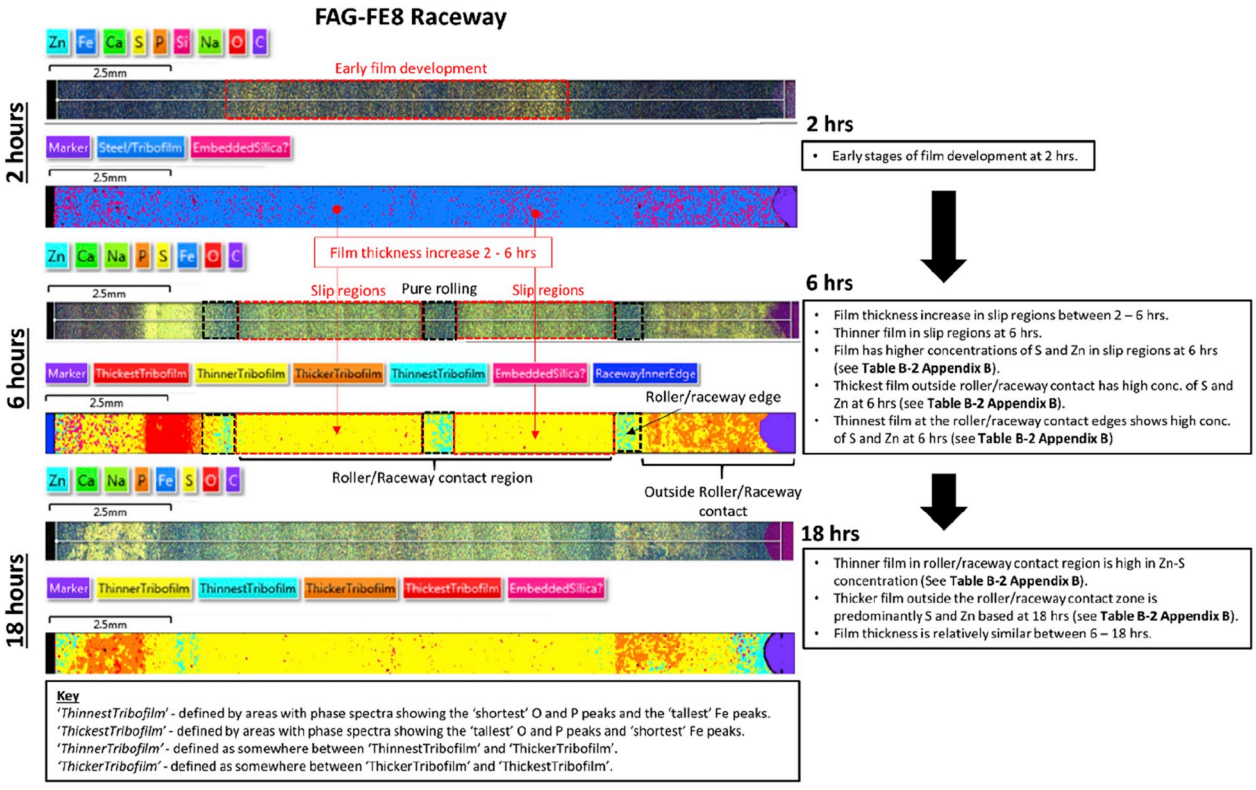

Fig. 14. EDX phase maps for Oil X raceways across 2, 6 and 18 h. Key explains difference between thickness terms.

no effect on the diffusion of hydrogen into the raceway, this potentially being due to the tribofilm formed on the raceway (discussed in **4.4**). For the OBCaSul (1.4%–5.6%) oils, there is a positive correlation between increase in OBCaSul wt% and increase in diffusible hydrogen concentration. Again, this could be due to the tribofilms formed (see **4.4** for further discussion), where it is considered that differences between oil chemistries (and respective tribofilms formed) could affect the flux/rate of hydrogen diffusion into the steel during operation. TDA results from set-up 2 showed that hydrogen diffused into the ZDDP only (OBCaSul 0%) and OBCaSul 5.6% oils (Table 5 and Fig. 9). TDA was not conducted on the OBCaSul 1.4% and 2.8% oils due to time considerations and so trends cannot be examined, further TDA on these oils should be conducted so that a comparative assessment can be made. Differences in measured hydrogen concentrations between roller and raceway may be due to.

(i) The differing dynamics experienced between roller and race, for example, number of contact cycles experienced and 'regeneration times' as mentioned above in **4.1.1.** However, regeneration times are slightly longer for the rollers than the raceways, where longer times are said to lead to longer WEC lives, only the raceways failing during FAG-FE8 testing [16]. This was said to be due to the higher asperity energy accumulation experienced by the raceways. This is contradictory to results found by the authors of this manuscript, where only the rollers contained WECs [18].
(ii) It may be due to differences in steel cleanliness, the raceway being shown to be far 'cleaner' than the rollers [18], thus a lack of trapping sites for hydrogen being available.
(iii) Differences in respective tribofilms formed on the roller and raceway (see **4.4** for further discussion).

Finally, differences in the water content measured between the tested oils (see Table 2) may play a role in the amount of diffusible hydrogen measured. Results show a correlation between increase in water content (ppm) measured in the oils pre-RCF testing, and an increase in diffusible hydrogen concentration measured in the rollers (see Fig. 8). The hygroscopic character of ZDDP, Na, Mg and Ca alkyl sulfonate additives may be a reflection on the increase in water content measured for the respective oils, where it is proposed that water dissociation and subsequent hydrogen generation due to high friction films formed by these additive components can occur [5]. Although water contents are low, small amounts of water as little as ~100 ppm have been shown to have a detrimental effect on fatigue life [48]. It has been said that water desorption spectra should be taken into account when measuring the total amount of diffusible hydrogen in steels, where thermal desorption and XPS analysis showed that the permeation of hydrogen is strongly influenced by the formation of oxide and/or hydroxide film when water is present [13]. It is noted, however, that when water is present hydrogen is mainly sourced from the oil opposed to water [49].

The trapping behaviour of hydrogen is discussed in Fig. 15 below.

4.3. Hydrogen diffusion and its relation to WEC formations

Discussions are focused on FE8 testing only.

While the diffusible hydrogen concentrations are comparable in the tests lubricated by the Oil X and OBCaSul oils, the number of WECs recorded in the rollers are significantly different, i.e. the concentration of diffusible hydrogen found in rollers lubricated by different oils may not have had the same effect on WEC formation, where minute differences or similar diffusible hydrogen concentration between rollers 'with' and 'without' WECs between the tested oils are found. Comparing for example TDA results for Oil X at 12 h and OBCaSul 1.4% at 18 h (Fig. 8). Although the average hydrogen concentrations are similar, no WECs were recorded in the 1.4% OBCaSul rollers while a number of WECs were found to have formed in the Oil X 12 h rollers (see Ref. [18] for Oil X 12 h WEC details). Again, if we compare diffusible hydrogen concentrations between Oil X and OBCaSul 5.6% (at 18 h), although their average hydrogen concentrations are similar, there is a vast difference in the number of WECs recorded (Table 4 and Fig. 6). This supports the suggestion made in a previous study by the authors, that hydrogen may not be an initiator but an accelerator to WEC formation

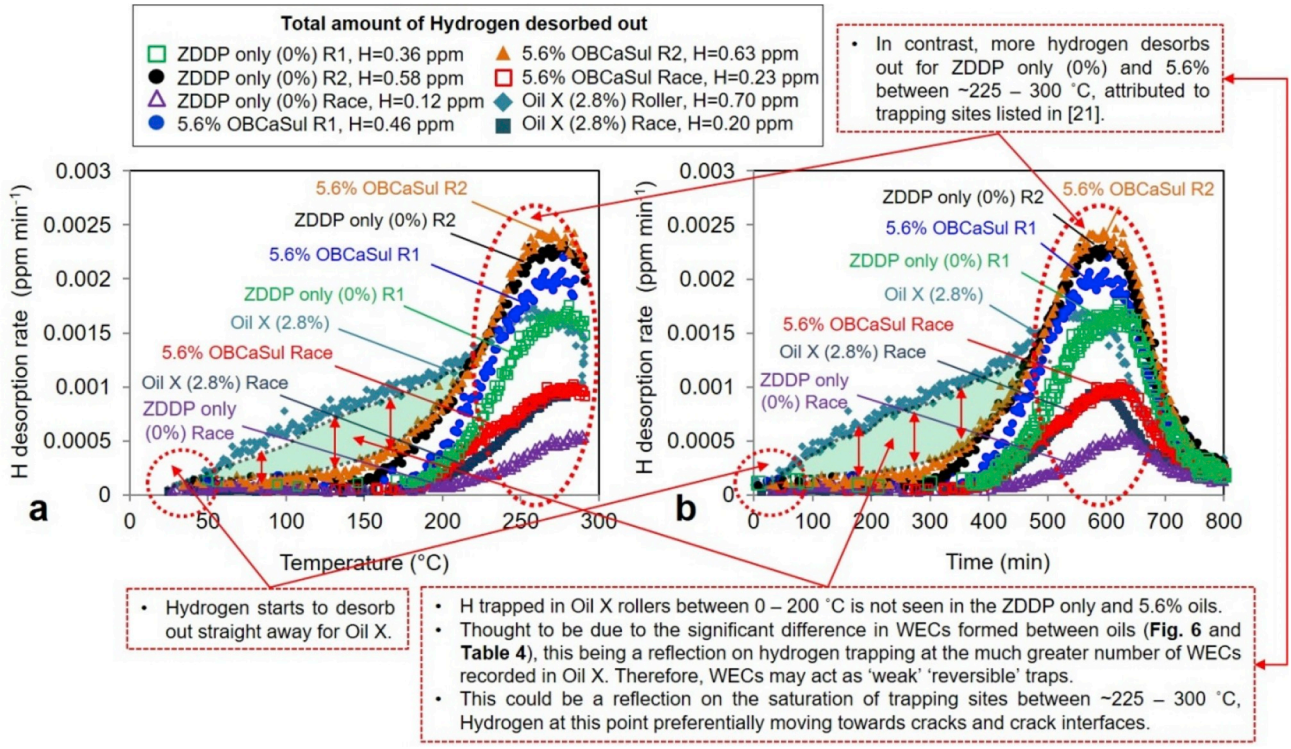

Fig. 15. Trapping behaviour of hydrogen in FAG-FE8 tested rollers and raceways analysed through TDA set-up 2.

[21], and/or becomes instrumental in formation when in combination with other factors e.g. tribofilm formed. It is noted that, at this stage, it is not clear what the influence of local diffusible hydrogen, i.e. at crack tips or inclusions, may have due to the limitation of the TDA, which only measures diffusible hydrogen in the bulk of the specimens. It is also considered that differences in oil chemistries may affect the flux/rate of hydrogen diffusion and penetration, this being directly related to the respective tribofilms formed (further discussion in **4.4**). It could be that.

(i) Hydrogen diffused later towards the end of RCF operation, not allowing a sufficient amount of time for hydrogen to take effect. Further TDA to measure diffusible hydrogen at varying stages of RCF operation for the OBCaSul oils (test run to only 18 h for these oils) would be able to provide more detail on this.
(ii) Hydrogen penetration may be outside the zones of maximum subsurface shear stresses, or where critical inclusions are located in the depth of the steel.
(iii) Insufficient hydrogen diffusion in critical zones where greater propensity for WEC formations exists, the diffusion of hydrogen in these zones being governed by the presence of metal-containing additives in the film such as calcium sulfonates under high frictional energy accumulation [44].

A difference in hydrogen trapping behaviour is seen between Oil X, and the ZDDP only (OBCaSul 0%) and OBCaSul 5.6% oils (Fig. 15). This may be a result of the greater number of WECs formed in the Oil X lubricated rollers in comparison, where it is suggested that crack interfaces have acted as 'weak' 'reversible' hydrogen traps.

Based on the TDA and serial sectioning analysis, a positive correlation is shown between the OBCaSul concentration and the amount of diffusible hydrogen. In addition, a jump in diffusible hydrogen concentration is seen for a jump in WEC formations between OBCaSul 1.4% and 2.8%, further TDA and serial sectioning for OBCaSul wt% between 1.4% and 2.8% is recommended to explore this. An increase in hydrogen concentration is seen between OBCaSul 2.8% and 5.6%, however, no great difference in number of WECs was seen, although the length of WECs formations increased. TDA was not conducted on the MPR rollers due to time constraints and so it is not possible to derive this relationship for the MPR tests, further testing is thus required to make a comparative assessment. The vast majority of WECs recorded for the OBCaSul FE8 tested oils were contained entirely within the subsurface. This supports previous findings by the authors on FAG-FE8 testing lubricated with Oil X [21], that the suggested mechanism of hydrogen entry into the steel during operation is at wear induced nascent surfaces or areas of heterogeneous tribofilm, hydrogen being generated by decomposition of lubricant through catalytic reactions and/or tribo-chemical reactions of water [12,13].

4.4. Influence of oil chemistry on tribofilm formation

4.4.1. Tribofilm composition

Discussions below focus on SEM/EDX analysis of the tribofilm from the FE8 tests only.

SEM/EDX has shown that the OBCaSul (1.4%–5.6%) oils have formed thicker Ca dominated films across wear zones on the rollers in comparison to 'normal' Zn−S films that are shown to form for the ZDDP only (OBCaSul 0%) rollers and raceways, and the Oil X and OBCaSul (1.4%–5.6%) raceways. For Oil X, an increase in RCF test duration has also resulted in thicker Ca films forming across wear zones on the rollers. ZDDP + OBCaSul combinations have shown that surfaces covering worn areas showed mainly Ca and O in the film [32], the Oil X and OBCaSul (1.4%–5.6%) lubricated rollers in this study exhibiting this behaviour. AES has shown that by using neutral calcium sulfonate with ZDDP, films contained Ca but were otherwise similar to ZDDP, the OBCaSul showing Ca and O with no traces of ZDDP in the film and having a greater effect on the AW properties [32]. The dominance of Ca over Zn shown on the rollers is suggested to be a reflection of OBCaSul additive being a 'strong' competitor to ZDDP in the oil. It is proposed that a replacement of Zn in the anti-wear tribofilm has resulted in thicker Ca films forming on the rollers. Ca replacement of Zn has been shown using multiple techniques on the analysis of automotive AW tribofilms on cam/tappet friction test specimens [35] and other engine parts [34].

As shown in Fig. 10, for Oil X at 2 h, the elements in the film are sporadically dispersed across the roller, while a well formed ZDDP tribofilm is shown to have developed on the raceway (indicated by the higher concentrations of Zn, S and P in the wear zones). In addition, the film thickness on the raceway is found to be thicker than that on the rollers at 2 h (see Fig. 11). Over time, while the film on the raceway does not change significantly, those on the rollers have developed and grow thicker, tribofilms on the raceway being on average thinner than the rollers. It is not clear why tribofilms form quicker on the raceway, but it may be an explanation for why no WECs were found to have formed in them. It is suspected that the differing contact dynamics between roller and raceway may affect film formation. For example, the rollers experience slightly longer 'regeneration times' (the time between subsequent contact load cycles) than the raceways, where longer regeneration times are said to improve resistance to WEC formation [16]. This is, however, contradictory to the results found in studies by the authors on FE8 tests using Oil X, where rollers contained multiple WECs, the raceway sections not showing any [18]. It is considered that longer regeneration times could influence film formation [16], which may be a reason as to why differences in tribofilm have been found in this study. More recently, it has been proposed that high surface shear forces in sliding areas due to the tribofilm formed (heterogeneous films composed of AW/EP and detergent/rust inhibiting additives) caused the initiation of surface cracks in FE8 RCF tested raceway samples [17].

4.4.2. Tribofilm formation influence on H-diffusion and WEC formations

TDA showed a positive correlation between OBCaSul wt% and diffusible hydrogen concentration for the FE8 rollers (see Table 5 and Fig. 9), where OBCaSul in oils containing ZDDP have formed thick Ca films. Therefore, it is suggested that the thick Ca films formed on the FE8 rollers have promoted hydrogen diffusion into the bearing steel. For Oil X an increase in RCF test duration also resulted in thicker Ca films forming, this being correlated with an increase in diffusible hydrogen concentration and WEC formations in the FE8 rollers. Based on TDA and serial sectioning analysis of the FE8 raceways, negligible hydrogen concentrations were detected and no evidence of WECs found, therefore, it is considered that the thinner Zn−S containing films formed on the raceways has demoted hydrogen diffusion and WEC formations.

Literature reports that an oil containing OBCaSul resulted in WEC detection (using ultrasound) in FE8 raceways, XPS/SNMS analysis showing increased film thickness (reaching 100 nm) over test duration and comprising of Ca−P on the raceway slip zones [2]. In contrast, removing OBCaSul resulted in no WEC detection, the developed film being thinner (20 nm) and comprising of Zn−S in the same regions. It must be noted that these tests used ceramic rollers to 'push' WEC failure to the raceways. ZDDPs are shown to reduce hydrogen permeation into steel, where it is suggested that these additives can form protective film preventing hydrogen permeation [50]. Studies in literature also propose that OBCaSul inhibit film formation and create 'weakened' heterogeneous ZDDP films [24–30], OBCaSul being suggested to promote and prolong nascent metal exposure [31].

In literature, STEM analysis shows heterogeneous tribofilms containing Ca, S, Zn, P, Na and O with varying thickness (5–100 nm) to

form on FE8 raceways that also showed WECs [17]. These elements were also observed on the roller films, where the study notes that the morphology and composition are different to the raceways, however, limited results are presented. It is worth mentioning that the rollers were not examined for damages since the majority of damage was found on the raceway surfaces, this contradicts what the authors of this study have seen on FE8 bearings using Oil X, where damage is only seen on the rollers [1,18].

Finally, it has been shown that for higher water contents (ppm) measured in the tested oils pre-RCF testing, higher diffusible hydrogen concentrations were measured (see Fig. 8). Water dissolved in the oil is said to influence the functionality of ZDDP AW additives and enhance wear [51–54]. A feature of ZDDP, and Ca alkyl sulfonate is that they are hygroscopic, where these additives may carry water molecules to rubbing contact surfaces [5]. MTM-Slim studies have shown oils containing ZDDP, Na, Mg and Ca alkyl sulfonates form thick patchy tribofilm, which are proposed to cause high friction in an initial incubation period (~20 h for FE8) resulting in water dissociation at fresh nascent surfaces and subsequent generation of hydrogen that diffuses into the steel promoting WEC formations [5].

Mechanisms for why Ca tribofilms are thicker than the Zn−S tribofilms and why these films may promote/demote hydrogen diffusion is still unclear based on the SEM/EDX analysis. Further tribofilm analysis using XPS and STEM has been conducted by the authors (to be published in a later study) and may be able to provide more information on the properties of the tribofilms and reveal physical mechanisms further. One answer may be that sulphonates can act as hydrogen poisoners, meaning that they can inhibit the recombination of hydrogen atoms (or radicals) to molecular hydrogen, hydrogen ions that then exist at the contact surface can recombine with electrons at fresh nascent metal surfaces forming atomic hydrogen that can diffuse into the steel [11]. Adding to this effect, it is also proposed that due to OBCaSul wanting to keep surfaces clean and prevent deposits at the contacting surface, the exposure of fresh nascent metal surfaces is proposed to be heightened [31].

5. Conclusions

RCF testing has been conducted under non-hydrogen charged conditions on FAG-FE8 and MPR rigs using 100Cr6 steel samples lubricated with oils containing varying wt% of OBCaSul detergent additive. The effects that oils containing OBCaSul have on tribofilm formation, diffusion of hydrogen into the steel, and the formation of WECs has been investigated. The findings of this study are:

- Serial sectioning has shown that WECs can initiate and propagate entirely within the subsurface and are frequently found to interact with small/short non-metallic inclusions. This has confirmed and added further verification to the author's previous findings.
- The number of WECs formed in the FE8 rollers appears to be increasing with the increase of OBCaSul wt% from 1.4% at 0 WEC, to 2.8% and 5.6% at 17 and 12 WECs respectively, suggesting that OBCaSul has promoted WEC formation. However, in the MPR tested rollers, only the OBCaSul 1.4% lubricated roller showed WECs, higher OBCaSul wt% (2.8% and 5.6%) not creating any potentially due to their differences in contact dynamics.
- Similar to the results obtained by FAG-FE8 testing using the fully formulated 'bad' oil (Oil X), TDA has also shown hydrogen to have diffused into the FE8 rollers and not the raceways during RCF operation for the OBCaSul containing and ZDDP only oils. TDA has shown a positive correlation between OBCaSul wt% and concentration of diffusible hydrogen. Further TDA should be conducted on the MPR rollers to confirm this relationship.
- Detailed tribofilm analysis has shown that oils containing OBCaSul additive form thicker Ca dominated tribofilms on the FE8 rollers as opposed to the normal Zn−S dominated tribofilm. This may have promoted hydrogen diffusion and WEC formations in the FE8 rollers. Thinner Zn−S containing films have been found to form on the FE8 raceways however, and these may have demoted hydrogen diffusion and WEC formations.

Acknowledgements

The authors would like to thank the sponsor of this study Afton Chemical for running the FAG-FE8 and MPR testing. The authors would also like to thank Grant Pollard, Afton Chemical, for facilitating the SEM/EDX tribofilm analysis. Thanks also to Sally Day, The Welding Institute (TWI) for facilitating TDA under set-up (1), and Steve Ooi for facilitating TDA under set-up (2) at the University of Cambridge.

Appendix A

Rank 1: Strong evidence for butterfly initiated WECs.

(i) Orientation of wings (+ve or –ve) being consistent with the wings of independent butterflies found in the serial sectioning analysis (not in the WEC network). +ve or –ve wing orientation is determined by the over –rolling direction, a second pair of wings being formed upon reversal of the over-rolling direction after a certain period [55].
(ii) The crack/wing angle, this being mainly ~45° with a range of 0-60° for typical butterfly formations [56,57].
(iii) If the microstructural change morphology associated with the crack/wing is of a typical 'classic wing-like pattern'.

Rank 2: Possible butterfly initiation or strong likelihood of WEC initiation independent of butterfly.

(i) This is the case when crack initiation features are observed however, the characteristics of butterfly formation as stated in Rank 1 type damage features are not observed.

Rank 3: Crack has passed through the inclusion during crack propagation; inclusion can therefore potentially aid in the propagation however, the inclusion is not involved in the initiation process of a crack.

(i) Orientation of the crack when passing through the inclusion was in a radial or near radial direction.
(ii) The inclusion interaction location is somewhere along one of the radial (depth direction) cracks of the WEC. In addition, microstructural change may not be observed around the crack.
(iii) The inclusion interaction depth is in an area of low subsurface shear stress.
(iv) The inclusion is small and is located inside a zone of considerable microstructural change with no crack visibly connecting to the inclusion.

Appendix B

Table B1
Average normalised atomic concentration for the FAG-FE8 tested Oil X analysed by SEM/EDX

Test duration	Norm. O%		Norm. Na%		Norm. S%		Norm. Zn%		Norm. Ca%		Norm. P%		Avg. Tribofilm thickness (nm)	
	Roller	Race	Roller	Race	Roller	Race	Roller	Race	Roller	Race	Roller	Race	Roller	Race
2 h	71.07	73.7	1.42	2.25	6.57	4.53	3.83	5.21	13.15	11.53	4.00	2.79	15	57
6 h	59.42	49.18	3.80	1.76	4.92	14.5	6.64	18.51	16.10	8.46	9.12	6.20	162	135
18 h	55.56	47.01	3.81	2.32	5.81	15.48	8.11	21.73	18.89	7.27	6.82	4.64	157	95

Table B2
Normalised atomic concentration for EDX mapping of FAG-FE8 tested Oil X roller and raceways

Roller	Phase	Norm. O%	Norm. Na%	Norm. P%	Norm. S%	Norm. Ca%	Norm. Zn%
2 Hours	Tribofilm	66.97	0.00	4.68	7.54	15.47	5.20
	Roller Edges	94.07	1.40	2.85	0.00	0.00	1.57
6 Hours	Thick Tribofilm	54.60	4.38	12.13	3.86	17.46	7.57
	Medium Tribofilm	56.77	3.95	8.41	4.72	20.68	5.47
	Thin Tribofilm	64.35	0.00	3.68	8.63	16.23	7.11
	Roller Edges	79.75	3.27	3.71	3.68	0.00	4.41
18 Hours	Thick Tribofilm	54.26	3.93	8.23	4.70	22.47	6.39
	Thin Tribofilm	51.40	3.48	4.14	9.73	18.18	13.11
	Roller Edges	78.90	3.74	3.02	3.28	3.83	7.19
Raceway	Phase	Norm. O%	Norm. Na%	Norm. P%	Norm. S%	Norm. Ca%	Norm. Zn%
2 Hour	Steel/Tribofilm	20.46	0.81	1.03	1.50	4.04	1.50
	Embedded Silica?	23.84	0.87	1.00	1.44	3.92	2.11
	Marker	53.96	0.59	0.00	0.00	0.00	0.00
6 Hour	Thickest Tribofilm	31.29	0.00	6.74	25.33	2.44	28.08
	Thicker Tribofilm	32.66	0.00	4.73	15.49	2.59	18.85
	Thinner Tribofilm	26.82	1.20	3.61	6.87	5.74	9.21
	Thinnest Tribofilm	18.23	0.00	1.18	3.99	2.46	4.87
	Embedded Silica?	33.02	0.61	1.73	5.15	2.36	6.56
	Raceway Inner Edge	34.58	0.00	0.00	4.55	0.00	5.95
	Marker	51.39	0.00	1.50	4.83	0.00	6.75
18 Hour	Thickest Tribofilm	33.56	0.00	4.22	19.77	0.00	24.00
	Thicker Tribofilm	27.20	0.00	2.83	13.26	1.80	17.07
	Thinner Tribofilm	19.17	0.82	2.08	6.12	3.71	8.81
	Thinnest Tribofilm	11.81	0.00	0.42	2.26	0.00	3.33
	Embedded Silica?	21.80	0.80	1.75	5.15	4.31	7.40

Table B3
Average normalised atomic concentration for the FAG-FE8 tested OBCaSul oils analysed by SEM/EDX

Test Oil	Norm. O%		Norm. S%		Norm. Zn%		Norm. Ca%		Norm. P%		Average tribofilm thickness (nm)	
	Roller	Race	Roller	Race	Roller	Race	Roller	Race	Roller	Race	Roller	Race
ZDDP only (OBCaSul 0%)	61.47	59.21	7.10	11.16	19.11	17.21	0	1.06	12.31	11.34	137.2	167.7
OBCaSul 1.4%	57.36	45.85	5.46	16.47	9.72	21.45	16.87	10.4	10.59	5.83	225.9	129.7
OBCaSul 2.8%	57.75	44.02	6.00	17.94	7.60	21.94	21.59	10.76	7.07	5.33	200.1	127
OBCaSul 5.6%	60.59	46.49	6.12	18.87	5.87	16.89	19.53	11.56	7.89	6.19	218.8	134

Declarations of interest

None.

Funding

This work is supported by a UK EPSRC PhD studentship; and Afton Chemical.

References

[1] Evans M-H, et al. Confirming subsurface initiation at non-metallic inclusions as one mechanism for white etching crack (WEC) formation. Tribol Int 2014;75:87–97.
[2] Franke J, et al. Influence of tribolayer on rolling bearing fatigue performed on a FE8 test rig. TAE 19th international colloquium tribology. 2014.
[3] Gould B, Greco A. The influence of sliding and contact severity on the generation of white etching cracks. Tribol Lett 2015;60(2):29.
[4] Gould B, Greco A. Investigating the process of white etching crack initiation in

bearing steel. Tribol Lett 2016;62(2):26.
[5] Haque T, et al. Lubricant effects on white etching cracking failures in thrust bearing rig tests. Tribol Trans 2018:1–33.
[6] Holweger W. Progresses in solving White etching crack phenoma. Golden, Colorado: NREL-Gearbox Reliability Collaborative; 2014. p. 45.
[7] L'Hostis B, et al. Influence of lubricant formulation on rolling contact fatigue of gears – interaction of lubricant additives with fatigue cracks. Wear 2017;382–383:113–22.
[8] Meheux M, et al. Effect of lubricant additives in rolling contact fatigue. Proc Inst Mech Eng J J Eng Tribol 2010;224(9):947–55.
[9] Tamada K, Tanaka H. Occurrence of brittle flaking on bearings used for automotive electrical instruments and auxiliary devices. Wear 1996;199(2):245–52.
[10] Wan GTY, et al. The effect of extreme pressure (EP) lubricants on the life of rolling element bearings. Proc Inst Mech Eng J J Eng Tribol 1994;208(4):247–52.
[11] Thompson AW, Bernstein IM. The role of metallurgical variables in hydrogen-assisted environmental fracture. In: Fontana MG, Staehle RW, editors. Advances in corrosion science and technology. Boston, MA: Springer US; 1980. p. 53–175.
[12] Kohara M, Kawamura T, Egami M. Study on mechanism of hydrogen generation from lubricants. Tribol Trans 2006;49(1):53–60.
[13] Tanimoto H, Tanaka H, Sugimura J. Observation of hydrogen permeation into fresh bearing steel surface by thermal desorption spectroscopy. Tribol Online 2011;6(7):291–6.
[14] Evans MH, et al. Confirming subsurface initiation at non-metallic inclusions as one mechanism for white etching crack (WEC) formation. Tribol Int 2014;75:87–97.
[15] Holweger W. Influence on bearing life by new material phenomena. NREL-wind turbine tribology seminar. November 2011.
[16] Kruhöffer W, Loos J. WEC formation in rolling bearings under mixed friction: influences and “friction energy accumulation” as indicator. Tribol Trans 2017;60(3):516–29.
[17] Paladugu M, Lucas DR, Scott Hyde R. Effect of lubricants on bearing damage in rolling-sliding conditions: evolution of white etching cracks. Wear 2018;398–399:165–77.
[18] Richardson AD, et al. The evolution of white etching cracks (WECs) in rolling contact fatigue-tested 100Cr6 steel. Tribol Lett 2017;66(1):6.
[19] Ščepanskis M, Gould B, Greco A. Empirical investigation of electricity self-generation in a lubricated sliding–rolling contact. Tribol Lett 2017;65(3):109.
[20] Holweger W, et al. White etching crack root cause investigations. Tribol Trans 2015;58(1):59–69.
[21] Richardson AD, et al. Thermal desorption analysis of hydrogen in non-hydrogen-charged rolling contact fatigue-tested 100Cr6 steel. Tribol Lett 2017;66(1):4.
[22] Paladugu M, Hyde RS. Microstructure deformation and white etching matter formation along cracks. Wear 2017;390–391:367–75.
[23] Rounds FG. Additive interactions and their effect on the performance of a zinc dialkyl dithiophosphate. ASLE Trans 1978;21(2):91–101.
[24] Inoue K, Watanabe H. Interactions of engine oil additives. ASLE Trans 1983;26(2):189–99.
[25] Gegner J, Nierlich W. The bearing axial cracks root cause hypothesis of frictional surface crack initiation and corrosion fatigue driven crack growth. NREL wind turbine tribology seminar. 2011.
[26] Zhang J, Yamaguchi E, Spikes H. The antagonism between succinimide dispersants and a secondary zinc dialkyl dithiophosphate. Tribol Trans 2014;57(1):57–65.
[27] Fujita H, Spikes HA. Study of zinc dialkyldithiophosphate antiwear film formation and removal processes, Part II: kinetic model. Tribol Trans 2005;48(4):567–75.
[28] Matsui Y, Aoki S, Masuko M. Influence of coexisting functionalized polyalkylmethacrylates on the formation of ZnDTP-derived tribofilm. Tribol Int 2016;100:152–61.
[29] Topolovec-Miklozic K, Forbus TR, Spikes H. Film forming and friction properties of overbased calcium sulphonate detergents. Tribol Lett 2008;29(1):33–44.
[30] Yamaguchi ES, et al. Boundary film formation by ZnDTPs and detergents using ECR. Tribol Trans 1998;41(2):262–72.
[31] Liston TV. Engine lubricant additives what they are and how they function. Lubricat Eng 1992;48(5):389–97.
[32] Kapsa P, et al. Antiwear mechanism of ZDDP in the presence of calcium sulfonate detergent. J Lubricat Technol 1981;103(4):486–94.
[33] Wan Y, et al. Effects of detergent on the chemistry of tribofilms from ZDDP: studied by X-ray absorption spectroscopy and XPS. In: Dowson D, editor. Tribology series. Elsevier; 2002. p. 155–66.
[34] Smith GC, Bell JC. Multi-technique surface analytical studies of automotive antiwear films. Appl Surf Sci 1999;144–145:222–7.
[35] Willermet PA, et al. The composition of lubricant-derived surface layers formed in a lubricated cam/tappet contact II. Effects of adding overbased detergent and dispersant to a simple ZDTP solution. Tribol Int 1995;28(3):163–75.
[36] Costello MT, Urrego RA, Kasrai M. Study of surface films of crystalline and amorphous overbased sulfonates and sulfurized olefins by X-ray absorption near edge structure (XANES) spectroscopy. Tribol Lett 2007;26(2):173–80.
[37] Kasrai M, et al. Study of the effects of Ca sulfonate on antiwear film formation by X-ray absorption spectroscopy using synchrotron radiation. J Synchrotron Radiat 1999;6(3):719–21.
[38] Shirahama S, Hirata M. Proc. 5th int. Colloq. On additives for lubricants and operational fluids. Esslingen; 1986.
[39] Rounds F. Effect of detergents on ZDP antiwear performance as measured in four-ball wear tests. Lubricat Eng 1989;45(12):761–9.
[40] Ramakumar SSV, Rao AM, Srivastava SP. Studies on additive-additive interactions: formulation of crankcase oils towards rationalization. Wear 1992;156(1):101–20.
[41] Hamrock BJ, Dowson D. Minimum film thickness in elliptical contacts for different regimes of fluid-film lubrication. Proceedings of the 5th leeds-lyon symposium on tribology. 1979. p. 22–7. 1978.
[42] Hamrock BJ, Dowson D. Ball bearing lubrication: the elastohydrodynamics of elliptical contacts. New York: J. Wiley & Sons; 1981. p. 1981.
[43] ISO 3690:2012, Welding and allied processes - determination of hydrogen content in arc weld metal.
[44] Franke J, et al. White etching cracking—simulation in bearing rig and bench tests. Tribology Transactions; 2017. p. 1–11.
[45] Evans M-H, et al. Serial sectioning investigation of butterfly and white etching crack (WEC) formation in wind turbine gearbox bearings. Wear 2013;302(1–2):1573–82.
[46] Evans M-H, et al. Effect of hydrogen on butterfly and white etching crack (WEC) formation under rolling contact fatigue (RCF). Wear 2013;306(1–2):226–41.
[47] Evans M-H, et al. White etching crack (WEC) investigation by serial sectioning, focused ion beam and 3-D crack modelling. Tribol Int 2013;65:146–60.
[48] Schatzberg P, Felsen IM. Effects of water and oxygen during rolling contact lubrication. Wear 1968;12(5):331–42.
[49] Grunberg L, Jamieson D, Scott D. Hydrogen penetration in water-accelerated fatigue of rolling surfaces. Phil Mag 1963;8(93):1553–68.
[50] Tanaka H, et al. The effect of lubricant additives on hydrogen permeation under rolling contact. Tribol Lett 2017;65(3):94.
[51] Brizmer V, Pasaribu HR, Morales-Espejel GE. Micropitting performance of oil additives in lubricated rolling contacts. Tribol Trans 2013;56(5):739–48.
[52] Cen H, et al. Effect of water on ZDDP anti-wear performance and related tribochemistry in lubricated steel/steel pure sliding contacts. Tribol Int 2012;56:47–57.
[53] Soltanahmadi S, et al. Tribochemical study of micropitting in tribocorrosive lubricated contacts: the influence of water and relative humidity. Tribol Int 2017;107:184–98.
[54] Parsaeian P, et al. Study of the interfacial mechanism of ZDDP tribofilm in humid environment and its effect on tribochemical wear; Part I: Experimental. Tribol Int 2017;107:135–43.
[55] Tricot R, Monnot J, Lluansi M. How microstructural alterations affect fatigue properties of 52100 steel. Met Eng Q 1972;12(2):39–47.
[56] Evans M. White structure flaking (WSF) in wind turbine gearbox bearings: effects of ‘butterflies’ and white etching cracks (WECs). Mater Sci Technol 2012;28(1):3–22.
[57] Evans M-H. White structure flaking fsailure in bearings under rolling contact fatigue. University of Southampton; 2013.